POLITECNICO DI TORINO

Master of Science

in Aerospace Engineering

Master thesis

Sonoluminescence and near self-similar spherically symmetric solutions of Navier-Stokes and Euler equations

Supervisors

Prof. D. TORDELLA

(Politecnico di Torino DISAT)

Prof. G. STAFFILANI

(MIT Mathematics Department)

Candidate

Leonardo POLLINI

July 2021

Abstract

Sonoluminescence is a phenomenon that occurs when a bubble is excited by a driving sound wave with resonant frequency. The implosion is so strong that the internal energy is spatially concentrated of about twelve orders of magnitude in a small volume of a radius in the order of 10^{-6} meters. Concomitantly, emission of light is observed.
A deep comprehension of this phenomenon is yet to be reached, because of the complex interaction between the bubble wall dynamics and the interior chemistry and hydrodynamics.
In this work a comparison between the physical phenomenology and a recently found set of mathematical solutions to the spherically symmetric Navier-Stokes and Euler equations is conducted. The physical aspects are described through a classic Rayleigh-Plesset model for bubble dynamics, considering a polytropic behaviour inside the interface.
The results show a good fit of the analytical solutions to the numerical data near the collapse, and three pairs of coefficients' values are estimated for the analytical solutions.

Acknowledgements

Beh, che dire... sono stati 6 anni lunghi e faticosi e non sarei mai riuscito ad arrivare qui se non fosse per le persone che ho avuto intorno.

Per primi non posso non ringraziare i miei genitori Stefania e Roberto per il costante supporto giorno dopo giorno. Per motivi vari non hanno potuto portare a termine gli studi e quindi hanno sempre fatto di tutto per stimolarci e non farci arrendere nei mille momenti di debolezza che affrontiamo ogni giorno crescendo. Ringrazio le mie sorelline (perchè sempre ine rimarrete per me!!!) Giorgia e Camilla che seppur tra mille discussioni non mi hanno mai fatto mancare una buona dose di affetto e sane scazzottate fraterne.

Un immenso grazie va a tutti gli zii (diretti, acquisiti e acquisiti degli acquisiti e via dicendo) che sono stati per me come secondi genitori e a nonna Rosa, che con le sue scorte e provviste mi ha fatto mettere qualcosa sotto i denti anche durante le sessioni più matte e disperate.

Nonostante sia sempre stato il loro *falzo* preferito, non posso non ringraziare di cuore i miei *amichi* di *DePilatus*: Totò, l'avvocheto, Rai, Luca, Masca, Marina e Ale... Senza di voi compagni di innumerevoli battaglie non ce l'avrei fatta ad arrivare fin qui, e con loro chiaramente ringrazio anche Rudy, Fra, Ire e Boj. Compagni di avventure, vacanze, sessioni di studio e grigliate.

Un ringraziamento particolare al buon Andrea, che mi è stato accanto come un fratello soprattutto nei primi anni di università, ma non solo.

Un grazie speciale va a Giulia che negli ultimi 2 anni ha dovuto sorbirsi tutte le mie lamentele (che non sono state poche) ma che anche lei mi ha sempre aiutato e sostenuto.

Last but not least... Vorrei ringraziare le mie due relatrici, la professoressa Daniela Tordella e la professoressa Gigliola Staffilani che mi hanno costantemente seguito e guidato nella realizzazione di questa tesi.

Mi rende felice pensare che la mia carriera accademica finisce (almeno per ora) con il supporto di due professoresse, così come era cominciata quasi venti anni fa, con le due maestre, Rita e Antonella, a cui sono rimasto sempre legato e che quindi voglio ringraziare di cuore.

So che più che ringraziamenti, sembra un flusso di coscienza, ma ho voluto scrivere tutto così come mi veniva, senza tornare indietro a cambiare le cose, e quindi continuando su quest'onda voglio lasciare quest'ultima riga per gli altri 3 nonni, Marcello, Franco e Giuliana a cui penso sempre.

Leonardo

Torino, 5 Luglio 2021

Table of Contents

List of Tables

List of Figures

Chapter 1

Introduction

1.1 Sonoluminescence and bubbles

The phenomenon called sonoluminescence consists in the emission of short bursts of light emitted by an imploding bubble under particular conditions. Although many theories have been formulated, the mechanism of sonoluminescence is still unknown today and therefore an introduction to the world of bubbles is necessary to fully understand the phenomenology of the problem.

A bubble is a simple cavity of a substance within another one or of a substance trapped inside an interface that separates the inside from the outside. In nature there are many examples of bubbles which can be observed everyday, such as bubbles of air in water or in ice (fig.1.2), bubbles created by the *Snapping shrimp* to catch their prey, globules of resin produced by conifers and other kinds of trees and plants or even the lava bubbles originated from the volcanic gas trapped inside the magma.

The interest around the world of bubbles has grown during the centuries. In fact, they have been studied with different approaches: art, since the 16th century, and more recently in mathematics, physics, chemistry and other scientific subjects [44, 46].

Examples of the use of bubbles in art could be paintings, in which they have been used as a metaphor of the fragility of human life. Most of them depict young boys and girls blowing soap bubbles, as shown in the painting of Simeon Chardin titled

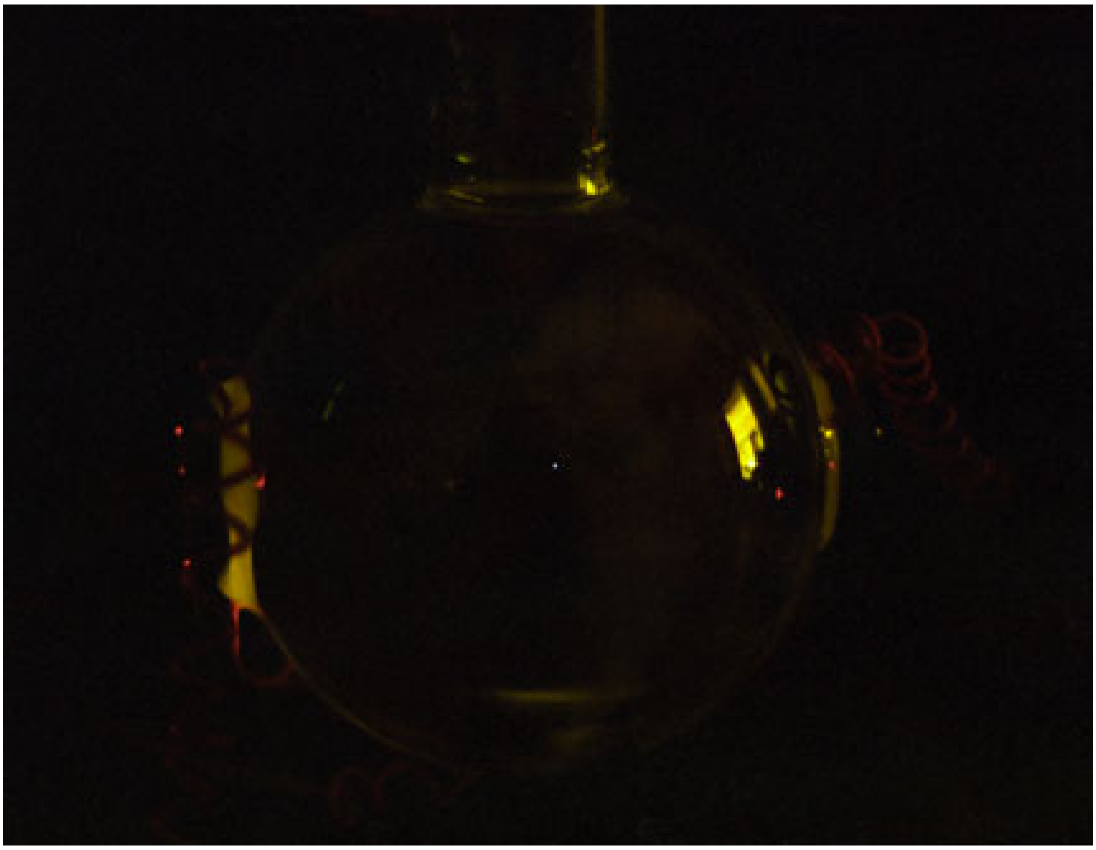

Figure 1.1: Sonoluminescing bubble in a flask of water

Les bulles de savon fig.1.3 (1733-34) or in the homonym painting of Édouard Manet fig.1.4 (1867).

Another important example of bubbles in art is music, in which they have been taken as the main topic of songs like *I'm forever blowing bubbles* by John Kellette (1918), today well known, especially in England, as the anthem of West Ham football club and as a part of the opening ceremony soundtrack of the 2012 London Olympics.

A more scientific approach to the bubbles world started after the derivation of the Navier-Stokes equations, in the 1840s, especially if reported in spherical coordinates. During the last 150 years many reaserchers have tried to understand the secrets hidden behind this curious phenomenon.

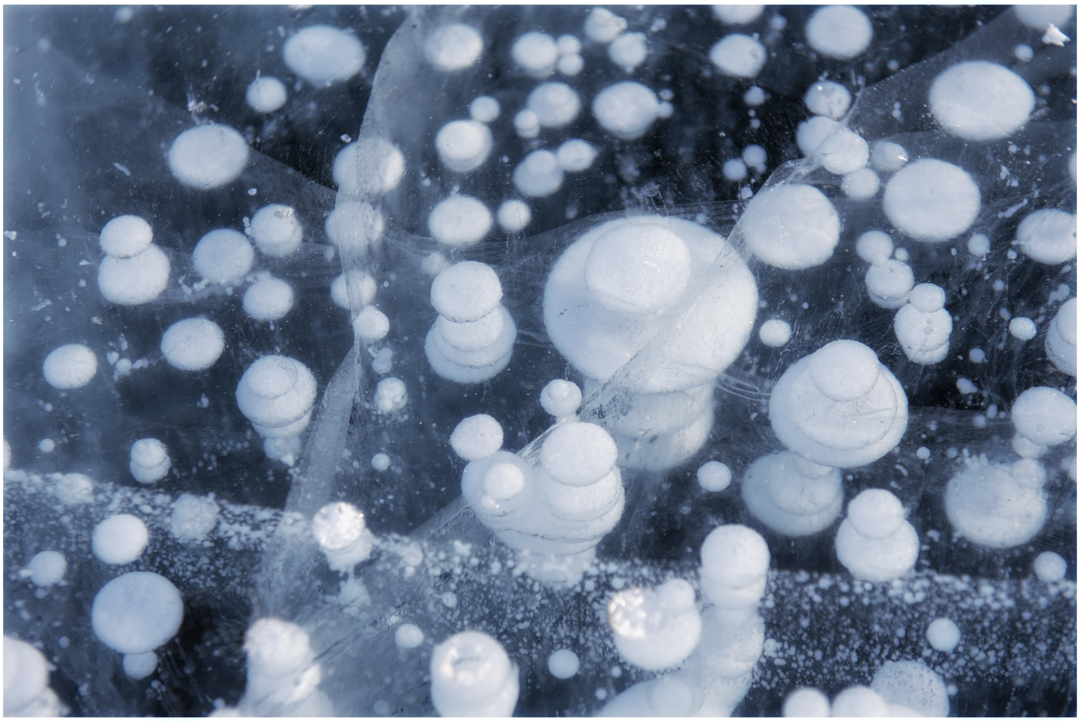

Figure 1.2: Air bubbles in the ice on Baikal Lake (Russia, 2018), courtesy of Raffaella Canfarini [53]

1.2 Thesis outline

In the reminder of this first section a brief historical overview and the objectives of this work are presented.
After that, the second section reviews some fundamentals of fluid dynamics, bubble dynamics and finally sonoluminescence, paying attention to the bubble's interior fluid dynamics and to the light emission models.
Section 3 contains the mathematical models and their analytical solutions which will then be used in section 4 for a comparision with the numerical solutions of the models presented in the second chapter.
Finally, section 5 contains a summary of the results obtained along with my opinions and some proposals for future works.

Figure 1.3: Les Bulles de savon, Jean-Baptiste Siméon Chardin (1733-34)

Figure 1.4: Les Bulles de savon, Édouard Manet (1867)

1.3 Historical background

In 1859, Besant published a first solution to the problem of the prediction of pressure and collapse time of a spherical bubble within an infinite mass of homogeneous, incompressible, inviscid fluid [1]. After that, in 1895 John Isaac Thornycroft, a Chief Constructor of the Royal Navy, introduced the term *cavitation* to describe the damage made by collapsing bubbles to ship propellers [2]. In order to understand this phenomenon, a theoretical analysis of this problem was made by Lord Rayleigh in 1917 who extended the problem of the collapse of both empty and gas-filled bubbles [3].
Starting from the Navier-Stokes equation, in 1949, Plesset derived a second order ODE that describes the dynamics of bubbles interface neglecting liquid viscosity, thermal effects and surface tension [7]. This equation was then generalized and refined by Poritsky in 1952, who added the liquid viscosity and proved that in absence of surface tension, the bubble doesn't collapse, and by Gilmore in the same year, who started to evaluate the effect of the compressibility of fluid

inside and outside the bubble [10, 9]. The latter was then developed by Tomita, Shima and Fujiwara in their works, in which they found a correlation between compressibility and damping, proving that the dynamics is significantly damped due to compressibility [15, 16, 17]. Subsequent important contributions were the development of stability theories that have allowed us to become aware of under what conditions the bubble would remain shape-stable [42, 31, 33].
Other refinements were made by Plesset, Prosperetti and others over a span of about 50 years and have been supported by numerical investigations mostly done by Werner Lauterborn [11, 12, 14, 8, 13].
As mentioned in *Single-Bubble Sonoluminescence*, light emission from collapsing bubbles was discovered in the early 1930s by Marinesco and Trillat (1933) and Frenzel and Schultes (1934) when they saw clouds of collapsing bubbles emit light [42, 4, 5]. This phenomenon, now called Multi-Bubble Sonoluminescence (MBSL), was considered just a consequence of the energy-focusing mechanism of cavitation and therefore it wasn't studied in depth until the discovery of Single-Bubble Sonoluminescence by Gaitan in 1989 [21, 22, 25].
Felipe Gaitan working with Larry Crum carried out many experiments using a flask of liquid and transducers to drive the bubble with an acoustic standing wave and they found the range of pressures and frequencies necessary to obtain SBSL.
After these first experiments many other physicists, mathematicians and engineers started searching for the causes of sonoluminescence. Always during 90s, Putterman and Barber carried out a set of experiments in order to understand how much SBSL focuses energy [23, 24]. Their works suggested that the pulse of light lasts much less than the common time scale of the compression and therefore the mechanism of SBSL is decoupled from the hydrodynamics of the bubble.
As reported in *Single-Bubble Sonoluminescence*, this result led to a bevy of ideas about the core mechanism of SBSL: Greenspan and Nadim (1993) suggested that the energy is focused by converging spherical shocks, Garcia and Levanyuk (1996) suggested the possibility of dielectric breakdown of the gas, Prosperetti (1997) suggested the so-called fracture-induced emission, Moss (1997) suggested the bremsstrahlung mechanism, Frommold and Atchley (1994) suggested the collision-induced emission and finally Eberlein (1996a,1996b) proposed the quantum-electrodynamical Casimir effect [28, 32, 35, 37, 30, 56, 57].

1.4 Objectives of this work

The main goal of this thesis is to supply a starting point for future analysis related to sonoluminescence, comparing new analytical solutions found by F. Merle, P. Raphael, I. Rodnianski and J. Szeftel to the Euler, Navier-Stokes and Non-Linear Schroedinger equations to the numerical and experimental solutions of the sonoluminescence models.
This can be done evaluating the asymptotical behaviour of the various solutions and fitting the obtained data. After this analysis, one can try to physically contextualize most of the properties derived from the mathematical approach and also try to transfer that from fluids to waves.

Chapter 2

Mathematical models for bubble dynamics

Bubbles dynamics requires to introduce the basic equations of fluid motion, the celebrated Navier-Stokes equations [48, 40, 19].

2.1 Fundamentals

In the derivation of these equations some assumptions are necessary:

- The fluid must be continuous, which implies that the Knudsen number has to be much smaller than one:

  $$\mathrm{Kn} = \frac{\lambda}{L} \ll 1$$

  This means that the mean free path of the molecules λ in a gas is much smaller than the characteristic length scale.

- The fluid has to be Newtonian, which implies a linear relation between the stress tensor and the symmetric part of the deformation tensor;

- The Stokes' hypotesis holds:

  $$\lambda = -\frac{2}{3}\mu$$

- The Fourier equation holds:
$$q_i = -k\frac{\partial T}{\partial x_i}$$

- The fluid has to be considered chemically non-reacting and homogeneous;

- Body forces are neglected;

- Radiation is neglected.

According to these hypoteses, the governing equations in differential, conservative form are:

$$\frac{\partial \rho}{\partial t} + \frac{\partial \rho u_j}{\partial x_j} = 0$$

$$\frac{\partial \rho u_i}{\partial t} + \frac{\partial \rho u_i u_j}{\partial x_j} = -\frac{\partial p}{\partial x_i} + \frac{\partial \tau_{ij}}{\partial x_j}$$

$$\frac{\partial E}{\partial t} + \frac{\partial (E+p)u_j}{\partial x_j} = -\frac{\partial(\tau_{ij}u_i - q_j)}{\partial x_j}$$

These equations express respectively, the mass conservation, the momentum conservation and the energy conservation inside the control volume. Where:

$$\tau_{ij} = \lambda\frac{\partial u_k}{\partial x_k}\delta_{ij} + \mu\left(\frac{\partial u_i}{\partial x_j} + \frac{\partial u_j}{\partial x_i}\right)$$

$$\bar{\bar{\tau}} = \begin{bmatrix} \tau_{xx} & \tau_{xy} & \tau_{xz} \\ \tau_{yx} & \tau_{yy} & \tau_{yz} \\ \tau_{zx} & \tau_{zy} & \tau_{zz} \end{bmatrix}$$

Neglecting all the viscosity terms it is possible to write the Euler equations:

$$\frac{\partial \rho}{\partial t} + \frac{\partial \rho u_j}{\partial x_j} = 0$$

$$\frac{\partial \rho u_i}{\partial t} + \frac{\partial \rho u_i u_j}{\partial x_j} + \frac{\partial p}{\partial x_i} = 0$$

$$\frac{\partial E}{\partial t} + \frac{\partial (E+p)u_j}{\partial x_j} = 0$$

Taking the curl of the momentum equation of the Navier-Stokes one can easily derive the vorticity equation:

$$\frac{\partial \omega_i}{\partial t} + u_j \frac{\partial \omega_i}{\partial x_j} = \omega_j \frac{\partial u_i}{\partial x_j} + \nu \frac{\partial^2 \omega_i}{\partial x_j \partial x_j}$$

These set of equations are presented in Cartesian coordinates, but for the analysis of a bubble, it is needed to write them in spherical coordinates [43, 20].

$$\frac{\partial \rho}{\partial t} + \frac{1}{r^2}\frac{\partial(\rho r^2 u_r)}{\partial r} + \frac{1}{r\sin\theta}\frac{\partial(\rho u_\theta \sin\theta)}{\partial \theta} + \frac{1}{r\sin\theta}\frac{\partial(\rho u_\phi)}{\partial \phi} = 0$$

$$\begin{aligned}\rho\left(\frac{\partial u_r}{\partial t} + u_r\frac{\partial u_r}{\partial r} + \frac{u_\theta}{r}\frac{\partial u_r}{\partial \theta} + \frac{u_\phi}{r\sin\theta}\frac{\partial u_r}{\partial \phi} - \frac{u_\theta^2 + u_\phi^2}{r}\right)&\\ = -\frac{\partial P}{\partial r} + \mu\left(\frac{\partial}{\partial r}\left(\frac{1}{r^2}\frac{\partial}{\partial r}\left(r^2 u_r\right)\right) + \frac{1}{r^2\sin\theta}\frac{\partial}{\partial \theta}\left(\sin\theta\frac{\partial u_r}{\partial \theta}\right)\right.&\\ \left. + \frac{1}{r^2\sin^2\theta}\frac{\partial^2 u_r}{\partial \phi^2} - \frac{2}{r^2\sin\theta}\frac{\partial}{\partial \theta}(u_\theta\sin\theta) - \frac{2}{r^2\sin\theta}\frac{\partial u_\phi}{\partial \phi}\right)&\end{aligned}$$

And:

$$\frac{\partial \rho}{\partial t} + \frac{1}{r^2}\frac{\partial(\rho r^2 u_r)}{\partial r} + \frac{1}{r\sin\theta}\frac{\partial(\rho u_\theta \sin\theta)}{\partial \theta} + \frac{1}{r\sin\theta}\frac{\partial(\rho u_\phi)}{\partial \phi} = 0$$

$$\rho\left(\frac{\partial u_r}{\partial t} + u_r\frac{\partial u_r}{\partial r} + \frac{u_\theta}{r}\frac{\partial u_r}{\partial \theta} + \frac{u_\phi}{r\sin\theta}\frac{\partial u_r}{\partial \phi} - \frac{u_\theta^2 + u_\phi^2}{r}\right) = -\frac{\partial P}{\partial r}$$

And for the vorticity:

$$\frac{\partial \omega_r}{\partial t} + (\mathbf{u}\cdot\nabla)\omega_r - (\omega\cdot\nabla)u_r) = 0$$

$$\frac{\partial \omega_\theta}{\partial t} + (\mathbf{u}\cdot\nabla)\omega_\theta - (\omega\cdot\nabla)u_\theta) + \frac{\omega_r u_\theta}{r} - \frac{\omega_\theta u_r}{r} = 0$$

$$\frac{\partial \omega_\Phi}{\partial t} + (\mathbf{u}\cdot\nabla)\omega_\Phi - (\omega\cdot\nabla)u_\Phi) + \frac{\omega_r u_\Phi}{r} - \frac{\omega_\Phi u_r}{r} + \frac{\omega_\theta u_\Phi\cot\theta}{r} - \frac{\omega_\Phi u_\theta\cot\theta}{r} = 0$$

Starting from the Euler equations in spherical coordinates, in the next paragraph, the equation for the bubble dynamics is derived.

2.2 Rayleigh-Plesset equation

The so called Rayleigh-Plesset (RP) equation is an ODE that controls the dynamics of a spehrical bubble in an infinite incompressible fluid field whose temperature and pressure at a great distance from the bubble are $T_\infty = cost$ and $p_\infty(t)$ respectively [3, 7, 13, 45, 14] .
This equation can be derived from the NS equations under the assumption of spherical simmetry and his dynamic parameter is the time-dependent radius $R(t)$ of the bubble.
As reported in 1.3, Rayleigh supplied the solutions to the problem of collapsing

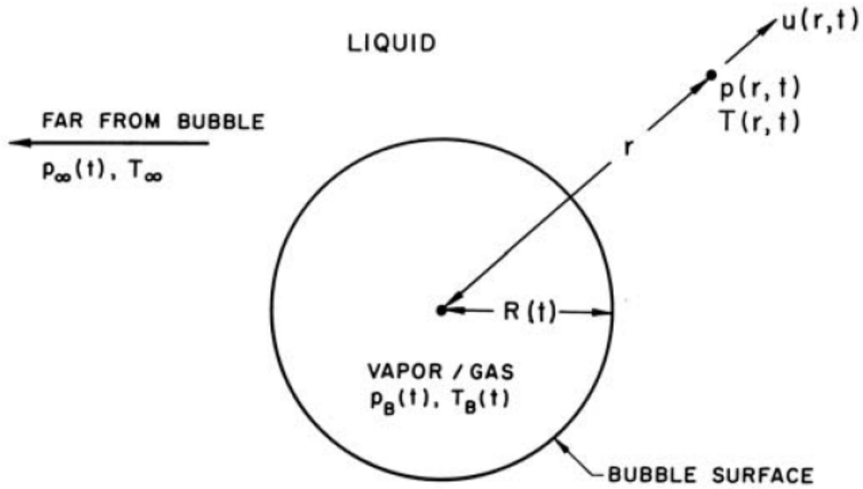

Figure 2.1: Spherical bubble in an infinite fluid field [45]

time and wall velocity [3]. Assuming that the whole kinetic energy of the motion is equals to the work done by the liquid, a bubble with an initial radius R_0 that collapses to R with velocity:

$$V = \sqrt{\frac{2}{3}\frac{p_\infty}{\rho_l}\left[\left(\frac{R_0}{R}\right)^3 - 1\right]}$$

and the time of collapse is given by direct integration from $R = R_0$ to $R = 0$:

$$\tau = 0.91468 R_0 \sqrt{\frac{\rho_l}{p_\infty}}$$

From this first results, Plesset in 1949, derived the equation for the bubble motion [7].
For the conservation of mass, the radial velocity must follow the inverse-square law

$$u(r,t) = \frac{F(t)}{r^2}$$

where $F(t)$ is a function of time related to the kinematic boundary condition. If we consider the ideal case of zero mass transport across the surface, the velocity become

$$u(r,t) = \frac{dR}{dt}$$

therefore the function $F(t)$ can be rewritten as

$$F(t) = R^2 \frac{dR}{dt}$$

Assuming that the fluid is Newtonian, the incompressible momentum balance equation for radial motion,

$$\frac{\partial u}{\partial t} + u \frac{\partial u}{\partial r} = -\frac{1}{\rho_l}\frac{\partial p}{\partial r} + \nu_l \left[\frac{1}{r^2}\frac{\partial}{\partial r}\left(r^2 \frac{\partial u}{\partial r}\right) - \frac{2u}{r^2}\right]$$

substituting $u(r,t)$:

$$-\frac{1}{\rho_l}\frac{\partial p}{\partial r} = -\frac{1}{r^2}\frac{dF}{dt} - \frac{2F^2}{r^5} = \frac{1}{r^2}\left(2R\left(\frac{dR}{dt}\right)^2 + R^2 \frac{d^2R}{dt^2}\right) - \frac{2R^4}{r^5}\left(\frac{dR}{dt}\right)^2$$

Note that during the substitution the viscous terms go to zero, in fact

$$\nu_l \left[\frac{1}{r^2}\frac{\partial}{\partial r}\left(r^2 \frac{\partial u}{\partial r}\right) - \frac{2u}{r^2}\right] = \nu_l \left\{ \frac{1}{r^2}\frac{\partial}{\partial r}\left[r^2 \left(\frac{-2F}{r^3}\right)\right] - \frac{2F}{r^4}\right\} = 0$$

This equation can be integrated from $r = R$ to $r \to \infty$ and the result is

$$\frac{p - p_\infty}{\rho_l} = R\frac{d^2R}{dt^2} + \frac{3}{2}\left(\frac{dR}{dt}\right)^2$$

It is necessary to construct the dynamic boundary conditions for the bubble surface. Considering a small portion of the bubble surface, the net force per unit area acting on this lamina can be written as the sum of the normal stress term, the surface tension term and the pressure :

$$\sigma_{rr}(R) + P_B - \frac{2S}{R}$$

where $\sigma_{rr} = -p + 2\mu_l \partial u/\partial r$ and S is the surface tension. And substituting the latter

$$-p + 2\mu_l\frac{\partial u}{\partial r} + P_B - \frac{2S}{R} = -p - \frac{4}{\mu_l}R\frac{dR}{dt} + P_B - \frac{2S}{R}$$

If the mass transport across the boundary is zero, this force per unit area must also be zero:

$$p(r = R) = p_B - \frac{4\mu_l}{R}\frac{dR}{dt} - \frac{2S}{R}$$

The result momentum equation becomes:

$$R\frac{d^2R}{dt^2} + \frac{3}{2}\left(\frac{dR}{dt}\right)^2 = \frac{p_B(t) - p_\infty(t)}{\rho_l} - \frac{4\nu_l}{R}\frac{dR}{dt} - \frac{2S}{\rho_l R}$$

This equation is the generalized RP equation for bubble dynamics by Plesset [7]. The closure of the model requires knowing the pressure inside the bubble. Assuming that the bubble contains a non-condensable gas with partial pressure p_{G_0} at some reference temperature T_∞ and size R_0, without any sort of mass transfer across the interface, it is possible to write:

$$p_B(t) = p_V(T_B) + p_{G_0}\left(\frac{T_B}{T_\infty}\right)\left(\frac{R_0}{R}\right)^3$$

Substituting this equation in the previous one, neglecting the thermal effect and assuming the temperature in the liquid uniform and the behaviour of the interior gas polytropic, the RP equation become:

$$R\frac{d^2R}{dt^2} + \frac{3}{2}\left(\frac{dR}{dt}\right)^2 = \frac{p_V(T_\infty) - p_\infty(t)}{\rho_l} + \frac{p_{G_0}}{\rho_l}\left(\frac{R_0}{R}\right)^{3k} - \frac{4\nu_l}{R}\frac{dR}{dt} - \frac{2S}{\rho_l R}$$

- The left hand side of the above equation is the inertial part. One can obtain an analytical solution by direct integration, that brings at the power law:

  $$R(t) = R_0[\frac{(t_s - t)}{t_s}]^{2/5}$$

  $$\dot{R}(t) \propto (t_s - t)^{-3/5} = \frac{1}{(t_s - t)^{3/5}}$$

  In the case of the bubble velocity is evident the diverging singularity for $t \to t_s$;

- On the right hand side, the first term represents the unbalance between the vapour pressure inside and the excitating pressure outside the bubble. The first one depends on the temperature inside the bubble that is supposed to be uniform and the same of the external liquid.
  The external pressure can be written in the form:

  $$p_\infty(t) = -p_a \sin(2\pi f t)$$

  Where f is the frequency and p_a is the amplitude of oscillations.

- The second term represents the polytropic behaviour of the gas inside the bubble, and it is a contribution of the assumption of non condensable gas;

- The third term represent the viscous effect, that is proportional to the bubble wall velocity and inversely proportional to the bubble radius, so one can note that this term become significant only for small radii;

- The last one represent the contribution of the surface tension, that is inversely proportional to the bubble radius, so this term become important only for small radii as viscosity.

One of the most important parameters involved in bubble dynamics is the exponent of the polytropic. As mentioned in *Single-bubble sonoluminescence*, the exponent

k of the polytropic depends on the phase of the bubble cycle: when the interface moves slowly, one can assume that the temperature inside the bubble is manteined constant and equal to the external liquid because the heat transfer is faster than the compression, so the transformation can be considered isothermal, with $\gamma = 1$; when the heat transfer process is slower than the bubble motion, the heat is not be able to be exchanged and so the bubble will behave adiabatically, with $\gamma = \Gamma$, that for a monoatomic gas is $\gamma = 5/3$ [42].
The parameters that can be used to distinguish these two situations is the Péclet number:

$$\mathrm{Pe} = \frac{|\dot{R}|R}{\chi_g}$$

where χ_g is the thermal diffusivity of the gas.
The equilibrium condition for a bubble can be easily derived by the Rayleigh-Plesset equation evaluating the initial condition $t = 0$ for which the derivatives go to zero and $p_\infty = p_\infty(0)$, so:

$$p_{G_0} = p_\infty(0) - p_V(T_\infty) + \frac{2S}{R}$$

Another important parameter is the resonant frequency, that can be calculated as:

$$f_0 = \frac{1}{2\pi}\sqrt{\frac{1}{\rho R_0^2}\left(3\gamma P_0 + (3\gamma - 1)\frac{2\sigma}{R_0}\right)}$$

According to this formula, a typical value of the resonant frequency for $R_0 \approx 5\mu m$ is of the order of $f_0 \approx 0.5MHz$ [45].

Others examples of models for the bubble dynamics are the Gilmore model and the Keller-Miksis model, both reported by Lauterborn and Kurz in the review *Physics of bubble oscillations* [9, 18, 47].
The Gilmore model takes into account the effects of sound radiation in the liquid from the oscillating bubble and it can be further refined with the Van der Waals hard core law. This model in his complete form is:

$$\left(1 - \frac{\dot{R}}{C}\right)R\ddot{R} + \frac{3}{2}\left(1 - \frac{\dot{R}}{3C}\right)\dot{R}^2 = \left(1 + \frac{\dot{R}}{C}\right)H + \frac{\dot{R}}{C}\left(1 - \frac{\dot{R}}{C}\right)R\frac{dH}{dR}$$

$$H = \int_{p|_{r\to\infty}}^{p|_{r=R}} \frac{dp(\rho)}{\rho}$$

$$p(\rho) = A\left(\frac{\rho}{\rho_0}\right)^{n_T} - B$$

$$p|_{r=R} = \left(p_{stat} + \frac{2S}{R_0}\right)\left(\frac{R_0^3 - bR_0^3}{R^3 - bR_0^3}\right)^k - \frac{2S}{R} - \frac{4\mu}{R}\dot{R}$$

$$p|_{r\to\infty} = p_{stat} + p_\infty(t)$$

$$C = \sqrt{c_0 + (n_T - 1)H}$$

Where c_0 is the sound velocity in the liquid at normal conditions, C is the the sound velocity at the bubble interface, H is the enthalpy, A, B and n_T are the parameters of the Tait equation of state and b is the constant of the Van der Waals hard core law.

Instead, the Keller-Miksis model takes into account the sound radiation in the liquid from the bubble with a retarded time $t - \frac{R}{c}$ and it reads as:

$$\left(1 - \frac{\dot{R}}{c}\right)R\ddot{R} + \frac{3}{2}\left(1 - \frac{\dot{R}}{3c}\right)\dot{R}^2 = \left(1 + \frac{\dot{R}}{c}\right)\frac{p_1}{\rho} + \frac{R}{\rho c}\frac{dp_1}{dt}$$

$$p_1 = \left(p_s tat - \frac{2S}{R_0}\right)\left(\frac{R_0}{R}\right)^{3k} - p_{stat} - \frac{2S}{R} - \frac{4\mu}{R}\dot{R} - p_\infty(t)$$

$$p_\infty(t) = p_a \sin(2\pi f t)$$

According to *Physics of bubble oscillations*, the three models presented give similar results, all of them very close to the experiments.

As reported by Brennen in *Bubble growth and collapse*, under the assumption of constant excitating pressure p_∞ and neglecting the viscosity, some analytical solutions can be found [45].

2.3 Sonoluminescence

It is clear that what has been described in the previous section is the starting point for a complete understanding of sonoluminescence. In fact, such phenomenon consists in the emission of short bursts of light emitted by an imploding bubble under particular conditions and the core dynamical equation is the RP equation. As mentioned in the paper *Defining the unknowns of sonoluminescence*, the interest in SL is because the energy enters the fluid by soundwave characterized by low energy and long wavelengths and comes out as bursts of light, which is at high energy [36]. This energy is concentrated by 12 orders of magnitude, in fact, typical acoustical energies are about 10^{-12} eV per molecule and classical light energies are around 1 eV [49, 36]. This behaviour cannot be described with the classical equations of fluid mechanics, therefore it is necessary to add equations for internal dynamics and light emission to the model.

2.3.1 Interior dynamics

Light emission strongly depends on the temperature inside the bubble, and the latter also depends on the gas composition.
Clearly the best way to proceed in the evaluation of the interior fluid's evolution is to compute the full compressible Navier-Stokes equation [19, 42]:

$$\frac{\partial \rho}{\partial t} + \frac{\partial \rho u_j}{\partial x_j} = 0$$

$$\frac{\partial \rho u_i}{\partial t} + \frac{\partial \rho u_i u_j}{\partial x_j} = -\frac{\partial p}{\partial x_i} + \frac{\partial \tau_{ij}}{\partial x_j}$$

$$\frac{\partial E}{\partial t} + \frac{\partial (E+p) u_j}{\partial x_j} = -\frac{\partial (\tau_{ij} u_i)}{\partial x_j} - \frac{\partial}{\partial x_j}(K_g \frac{\partial T}{\partial x_j})$$

With:

$$\tau_{ij} = \lambda \frac{\partial u_k}{\partial x_k}\delta_{ij} + \mu \left(\frac{\partial u_i}{\partial x_j} + \frac{\partial u_j}{\partial x_i} \right)$$

Numerically speaking this approach results very heavy.
According to *Single-bubble sonoluminescence*, from the early 90s, many attempts of solution have been carried on. In 1993 Wu and Roberts presented their work

on the inviscid model [27]. Three years later, Vuong and Szeri, proposed a more complex model including dissipation phenomena that was further extended in 2000 by Storey and Szeri including water vapour phase changing [34, 39].

For the subsequent analysis of this work of thesis, it is important to briefly describe the inviscid models. In fact, the work of Wu and Roberts started from the idea that the high temperature are caused by a mechanism of shock focusing. This assumption have allowed a comparison with the analytical solution of collapse of an imploding sphere found by Guderley in 1942 [27, 6].
His result shows that the dynamic behaviour of the radius of the converging shock follow the law:

$$R(t) \sim (t_s - t)^{\alpha}$$

and the computed values of α are respectively $\alpha \approx 0.6884$ and $\alpha \approx 0.7172$ for $\Gamma = 5/3$ and $\Gamma = 7/5$.
Considering an ideal gas equation of state is evident that, when $t \to t_s$, the temperature blow up. This behavior has to be attributed to having neglected the viscosity and thermal diffusion that make the model non-physical and this is the reason for the subsequent analyses of the dissipative models.

The main result of the analyses of the dissipative models, started with the work of Vuong and Szeri, is the absence of shock in argon and nitrogen bubbles [34, 38]. After a few years of research, Lin and Szeri reported the difficulties of formation of shock waves inside the sonoluminescing bubbles due to adverse entropy gradients and the weakening effect of the increasing sound speed towards the center [41].

Thanks to the direct analysis of the full gas-dynamical equations, it has been possible to state that all the thermodynamic parameters inside the bubble are slightly dependent of the space and therefore it is reasonable consider them only time-dependent [42]. This led to a different way to proceed in the computation of the internal temperature and pressure.
Assuming an adiabatic equation of state, with a van der Waals gas, and neglecting heat and mass transfer one can write the simplest possible model [29]:

$$p_G(t) = \left(P_0 + \frac{2S}{R_0}\right)\frac{(R_0^3 - h^3)^\Gamma}{(R(t)^- h^3)^\Gamma}$$

$$T_G(t) = T_0\frac{(R_0^3 - h^3)^{\Gamma-1}}{(R(t)^- h^3)^{\Gamma-1}}$$

These two equations are coupled with the classical RP equation.
The main problem in this case is the assumption of the adiabaticity, in fact, in the expansion phase of the bubble, the motion is so slow that allows heat exchange with the external liquid therefore the real behaviour is isothermal. One can correctly assumes an adiabatic behaviour in a restricted neighbourhood near the collapse.
The parameters that describes the change of behaviour is the Péclet number. Andrea Prosperetti in 1977 proposed a transition function $\gamma(\mathrm{Pe}(t))$, in order to insert a time-dependent polytropic coefficient in the model and this equation is included in the analysis made by Hilgenfeldt in 1999 [55, 59, 60]. The proposed equation for the temperature:

$$\dot{T} = -[\gamma(\mathrm{Pe}(t)) - 1]\frac{3R^2\dot{R}}{R^3 - h^3}T - (T - T_{w0})\chi_g/R^2$$

This model predict a peak temperatures in the order of $20000K$. Taking into account the heat and mass exchange the complexity of the problem goes up. In 1997, Yasui proposed a model based on the RP equation with a van der Waals gas inside that includes mass transfer through condensation and evaporation, and an heat exchange due to the latter cited phenomena and the temperature gradients. He also included in the model 25 possible chemical reactions for the water vapor [58].
His main result is that almost all the water is expelled during the collapse. The peak temperatures computed with this model reach only $10000K$ due to the heat absorption by the endothermical chemical reactions of the water vapor.
The main problem of this model is that Yasui has assumed that the transportation of mass through the interface is limited by the condensation. Some years later, in fact, has been proved that the limiting condition is the diffusion [39]. This statement was carried on in the paper *Suppressing dissociation in sonoluminescing bubbles: The effect of excluded volume* by Toegel et al., who evaluate the number

of molecules through the formula:

$$\dot{N_{H_2O}} = 4\pi R^2 D\partial|_{r=R} \approx 4\pi R^2 D\frac{n_0 - n}{l_{diff}}$$

with $l_{diff} = min[(RD/\dot{R})^{1/2}, R/\pi]$, where D is the gas diffusion constant.
The equation for the heat flux was:

$$\dot{Q} = 4\pi R^2 \chi_{mix}\frac{T_{w0} - T}{l_{diff}}$$

They also showed that the most important endothermical reactio is:

$$H_2O + 5.1eV \leftrightarrow OH + H$$

And this statement led to another equation for the temperature inside the bubble:

$$C_v\dot{T} = \dot{Q} - p_g\dot{V} + h_w\dot{N}^d_{H_2O} - \sum_X \frac{\partial E}{\partial N_X}\dot{N}_X$$

where X is the sum of the species.

Chapter 3

Analytical solutions (Merle, Raphaël, Rodnianski and Szeftel)

An important mathematical result about spherically-symmetric Euler and Navier-Stokes equations has been found in the latter years by F. Merle, P. Raphael, I. Rodnianski and J. Szeftel in the three companion papers [51, 52, 50].

3.1 Euler equations

In the first one, called *On smooth self-similar solutions to the compressible Euler equations*, the team of mathematicians showed the existence of such C^∞, global, self-similar solutions which, from smooth initial data, blow up in the origin at a certain moment $(T,0)$, with $T < \infty$ [51].
They moved from the previous works of Guderley, for whom the study of the solutions is reduced to the following system [6]:

$$\begin{cases} \frac{dw}{dx} = -\frac{\Delta_1}{\Delta} \\ \frac{d\sigma}{dx} = -\frac{\Delta_2}{\Delta} \end{cases}$$

Where Δ_1, Δ_2 and Δ are polynomials and the similarity variable $Z = e^x$ related to (t, y) through the relation:

$$Z = \frac{|y|}{(T-t)^{\frac{1}{r}}}$$

where r is dimentionally a speed.
Considering the compressible isentropic Euler equations:

$$\begin{cases} \partial_t \rho + \nabla \cdot (\rho u) = 0 \\ \rho \partial_t u + \rho u \cdot \nabla u + \nabla p = 0 \\ p = \frac{\gamma - 1}{\gamma} \rho^{\gamma} \\ \rho(t, y) > 0 \end{cases}$$

Introducing:

$$l = \frac{2}{\gamma - 1} > 0 \qquad r > 1$$

And the self-similar renormalization:

$$\begin{cases} \rho(t, y) = (\frac{\lambda}{\nu})^{\frac{2}{\gamma-1}} \widehat{\rho}(\tau, Z) \\ u(t, y) = \frac{\lambda}{\nu} \widehat{u}(\tau, Z) \\ Z = \frac{y}{\lambda} \\ \frac{d\tau}{dt} = \frac{1}{\nu} \\ -\frac{\lambda_\tau}{\lambda} = 1 \\ -\frac{\nu_\tau}{\nu} = r \end{cases}$$

It is now possible to renormalize the set of equations on $[0, T)$ as:

$$\begin{cases} \partial_\tau \widehat{\rho} + l(r-1)\widehat{\rho} + \Lambda \widehat{\rho} + \nabla \cdot (\widehat{\rho} \widehat{u}) = 0 \\ \partial_\tau \widehat{u} + (r-1)\widehat{u} + \Lambda \widehat{u} + \widehat{u} \cdot \nabla \widehat{u} + \nabla (\widehat{\rho}^{\gamma-1}) = 0 \\ \Lambda = Z \cdot \nabla \end{cases}$$

According to *On smooth self-similar solutions to the compressible Euler equations*, a self-similar profile is a stationary solution to the previous system [51]:

$$\begin{cases} l(r-1)\widehat{\rho} + \Lambda\widehat{\rho} + \nabla \cdot (\widehat{\rho}\widehat{u}) = 0 \\ (r-1)\widehat{u} + \Lambda\widehat{u} + \widehat{u} \cdot \nabla\widehat{u} + \nabla(\widehat{\rho}^{\gamma-1}) = 0 \end{cases}$$

with rate of concentration of the blow-up solution that is:

$$\lambda(t) = \lambda_0(T-t)^{\frac{1}{r}}$$

$$\nu(t) = r(T-t)$$

The solutions away from the concentration point (T,0) are:

$$\begin{cases} \rho(t,y) = \frac{1}{(T-t)^{(\frac{2(r-1)}{r(\gamma-1})}}\widehat{\rho}(Z) \\ u(t,y) = \frac{1}{(T-t)^{(\frac{(r-1)}{r}}}\widehat{u}(Z) \\ Z = \frac{y}{\lambda_0(T-t)^{\frac{1}{r}}} \end{cases}$$

With asymptotics:

$$\rho(t,y) = \frac{\rho_*(1 + o_{|Z|\to+\infty}(1))}{|y|^{\frac{2(r-1)}{r(\gamma-1)}}}$$

$$u(t,y) \sim \frac{u_*(1 + o_{|Z|\to+\infty}(1))}{|y|^{\frac{r-1}{r}}}$$

These solutions, lead to the existence of finite energy blow-up solutions of the Euler equations.
The importance of the solutions of this system of equations is that in the companion papers, these profiles have been used ad the leading order blow up profil [52, 50].

3.2 Navier-Stokes equations

As demonstrated in *On the implosion of a three dimensional compressible fluid* by Merle et al, considering the compressible, barotropic, three dimensionale Navier-Stokes equations [52]:

$$\begin{cases} \partial_t \rho + \nabla \cdot (\rho u) = 0 \\ \rho \partial_t u + \rho u \cdot \nabla u + \nabla p = \mu \Delta u + \mu' \nabla div(u) \\ p = \frac{\gamma - 1}{\gamma} \rho^\gamma \\ (\rho_{t=0}, u_{t=0}) = (\rho_0(x), u_0(x)) \in \mathbb{R}_+^* \times \mathbb{R}^3 \end{cases}$$

with $\rho > 0$, but which can decay at $+\infty$

$$\lim_{|x| \to +\infty} \rho(t, x) = 0$$

Defining the additional parameters:

$$l = \frac{2}{\gamma - 1}$$

$$r^*(d, l) = \frac{d + l}{l + \sqrt{d}}$$

$$r_+(d, l) = 1 + \frac{d - 1}{(1 + \sqrt{l})^2}$$

$$r_{\text{👁}}(d, l) = \begin{cases} r^*(d, l) \quad for \quad l > d \\ r_+(d, l) \quad for \quad l < d \end{cases}$$

Adopting the physical restriction on μ and μ':

$$\mu \geq 0 \qquad 3\mu' - \mu \geq 0$$

The main result obtained is the demonstration of the existence of a countable sequence $(l_n)_{n \in \mathbb{N}}$, with an accumulation point that can only be at $\{0{,}3, \infty\}$ such that, according to the previous defined parameters, and assuming that [52]:

$$l \neq 3$$

$$l > \sqrt{3}$$

for Navier-Stokes and

$$l > 3$$

for Euler. With:

$$l \notin \{l_n, n \in \mathbb{N}\}$$

For each possible l, there exists a discrete sequence of blow-up speeds $(r_k)_{k\geq 1}$ with:

$$1 < r_k < r_{\circledast}(3, l)$$

$$\lim_{k\to+\infty} r_k = r_{\circledast}(3, l)$$

such that the existence of a fintite co-dimensional group of smooth spherically symmetric initial data (ρ_0, u_0) such that the solutions to the NS and Euler equations blow-up in finite time $0 < T < +\infty$ at the center of symmetry is demonstrated for each $k \geq 1$, with:

$$||u(t,\cdot)||_{L\infty} = \frac{c_{u_0}(1 + o_{t\to T}(1))}{(T-t)^{\frac{r_k - 1}{r_k}}}$$

$$||\rho(t,\cdot)||_{L\infty} = \frac{c_{\rho_0}(1 + o_{t\to T}(1))}{(T-t)^{\frac{l(r_k - 1)}{r_k}}}$$

with $c_{u_0} > 0$ and $c_{\rho_0} > 0$ costants [52].
This set of solutions describe the self-implosion of a fluid due to some distribution of matter characterized by finite energy. These profiles reamin smooth until the blow up. It is important to note that these solutions do not describe self-similar profiles as in the Euler case.

3.3 Properties of solutions

The presented solution is characterized by some important peculiarities and properties [52].

- None of the parameters that characterize the solutions are dependent to the viscosity μ and μ';
- The value of $l > \sqrt{3}$ is fundamental for the compatibility of the Navier-Stokes solutions to the Euler-like blow up. In addition it is known that the this phenomenon happens only for $l = d$ where d is the general dimension;
- The above reported theorem that supply the solution holds for Euler in a bidimensional case;
- The sequence of the parameter l_n is strictly related to the existence of C^∞ self-similar solutions for Euler;
- One of the hypotesis is that the behaviour at infinity of ρ and u is known a priori because the should decay and this involves that the energy of the solutions is finite;
- The solutions are valid for spherically symmetric initial data, but they are also stable for non-symmetric perturbations;
- In contrast with the previous solutions to the shock formation problem, in this solution both velocity and density diverge at the time of the first singularity;
- The stability problem has yet to be fully treated;

Blow up solutions found by Merle et al are strictly connected with the solution at the singularity formation problem in defocusing super-critical Schrȯdinger equations.

3.4 Nonlinear Schrödinger equations

Considering the defocusing super-critical Schrödinger equation [50]:

$$i\partial_t u + \Delta u - u|u|^{p-1} = 0$$

$$u_{|t=0} = u_0$$

with:

$$(t, x) \in [0, T) \times \mathbb{R}^d, \qquad u(t, x) \in \mathbb{C}$$

in dimension $d \geq 3$ ancd with $p \in 2\mathbb{N}^* + 1$.

Merle et al. proposed a new set of solutions in the paper *On blow up for the energy super critical defocusing nonlinear Schrödinger equations* [50].
They demonstrate that for dimensions $5 \leq d \leq 9$ the equation admits a blow up solution from C^∞ initial data that is not related to the classical soliton or self-similar solutions.

Introducing:

$$(d, p) \in \{(5{,}9), (6{,}5), (8{,}3), (9{,}3)\}$$

and

$$r^*(d, l) = \frac{l + d}{l + \sqrt{d}}$$

$$l = \frac{4}{p - 1}$$

There exists a sequence of blow up speeds $(r_k)_{k\geq 1}$ with

$$2 < r_k < r^*(d, l)$$

$$\lim_{k\to+\infty} r_k = r^*(d, l)$$

such that the existence of a finite co-dimensional group of smooth spherically symmetric initial data u_0 such that the solution to the NLS blow up in finite time

$0 < T < +\infty$ at the center of symmetry is demonstrated for each $k \geq 1$, with:

$$||u(t,\cdot)||_{L\infty} = \frac{c_{p,r,d}(1 + o_{t\to T}(1))}{(T-t)^{\frac{1}{p-1}(1+\frac{r_k-2}{r_k})}}$$

with $c_{p,r,d} > 0$.

Chapter 4

Numerical simulations and results

The goal of this work of thesis is to compare the analytical solutions reported in the previous section to the numerical data of the Rayleigh-Plesset equation for bubble dynamics.
The equation used is:

$$\ddot{R} = -\frac{3}{2}\frac{\dot{R}^2}{R} + \frac{p_G}{\rho R} - \frac{p_0}{\rho R} + \frac{p_\infty(t)}{\rho R} + \frac{1}{\rho c}\frac{d}{dt}[p_G(R) + p_\infty(t)] - \frac{4\mu\dot{R}}{\rho R^2} - \frac{2S}{\rho R^2}$$

With:

$$p_\infty = P_A \sin(\omega t)$$

$$p_G = \frac{p_0 * R_0^{3k}}{(R^3 - a^3)^k}$$

$$T_G = \frac{T_0 * R_0^{3(k-1)}}{(R^3 - a^3)^{(k-1)}}$$

And it is reported in the MatLab function in Appendix A. The first phase of this analysis was characterized by numerous attemps to find the best settings for the following simulations. In fact, the first attemps, with explicit and implicit Euler and Runge-Kutta 4, led to numerical errors and divergent solutions. In the neighbourhood of the collapse the derivatives values change so rapidly that a time

step of 10^{-18} is required. Due to the computational cost, a variable time-step method has been used for the integration in simulink.
The model settings are reported in the following table:

Start time	$0.0s$
Stop time	$1/26500s$
Max step size	10^{-8}
Min step size	10^{-18}
Initial step size	Auto
Relative tolerance	10^{-3}
Absolute tolerance	Auto

Table 4.1: Simulation general settings

The initial data choose for the simulation are reported in the paper *Toward a hydrodynamic theory of sonoluminescence* by Löstedt, Barber and Putterman [29]. This choise has to be addressed to the version of RP equation used. In fact, they modified the classical version in order to include the damping due to the acoustical radiation for small mach numbers.

Initial radius	$R_0 = 4.5\mu m$
Liquid density	$1000kg/m^3$
Sound velocity in the liquid	$1481m/s$
Initial pressure	$101325Pa$
Initial temperature	$T_0 = 288K$
Dynamical viscosity	$3 \cdot 10^{-3}kg/(ms)$
Surface tension	$3 \cdot 10^{-2}kg/s^2$
Vand der Waals hard core	$a = R_0/8.54\mu m$
Polytropic exponent	$k = 5/3$
Driving sound wave amplitude	$p_A = 1.35atm$
Excitation frequency	$f = 26500Hz$
Pulsation	$\omega = 2 * \pi * 26500rad^{-1}$

Table 4.2: Initial data

In figure 4.2 is reported a classical solution to the RP equation obtined by Löstedt, Barber and Putterman [29]. The simulink model used for this analysis is the following:

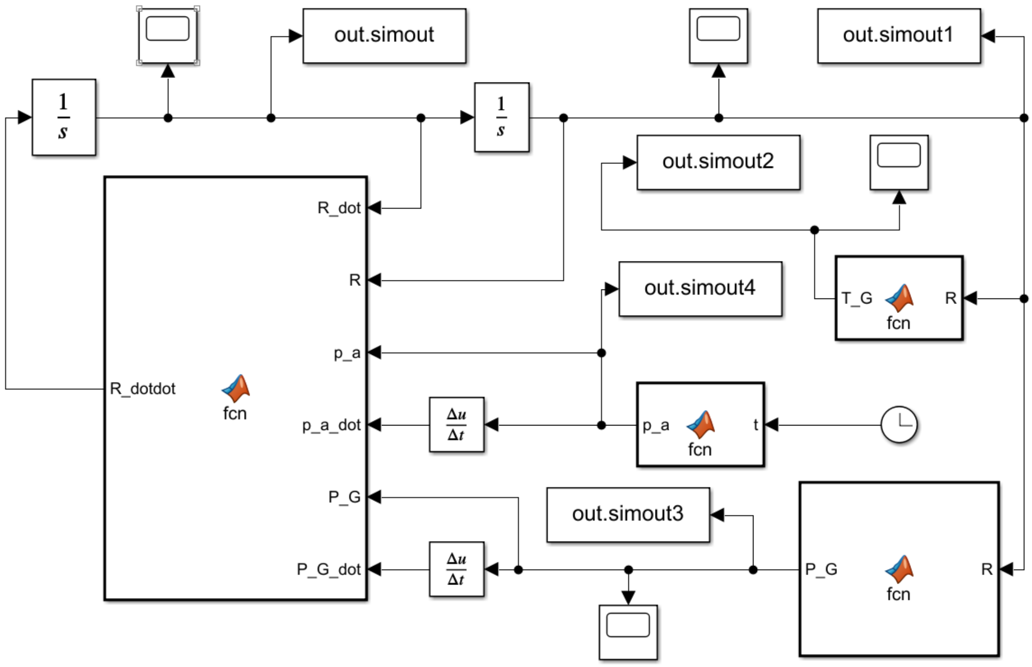

Figure 4.1: Bubble dynamics. Rayleigh-Plesset representation model and related algorithm to obtain solutions under spherical symmetry. Simulink associated flow chart. See Appendix A

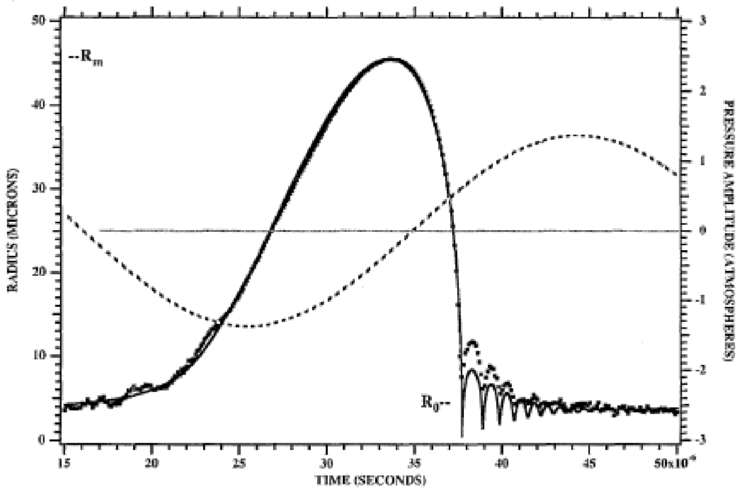

Figure 4.2: Radius dynamics by Löstedt, Barber and Putterman [29]

Launching the file called *Main_6.m* one can easily obtain the following plots for bubble:

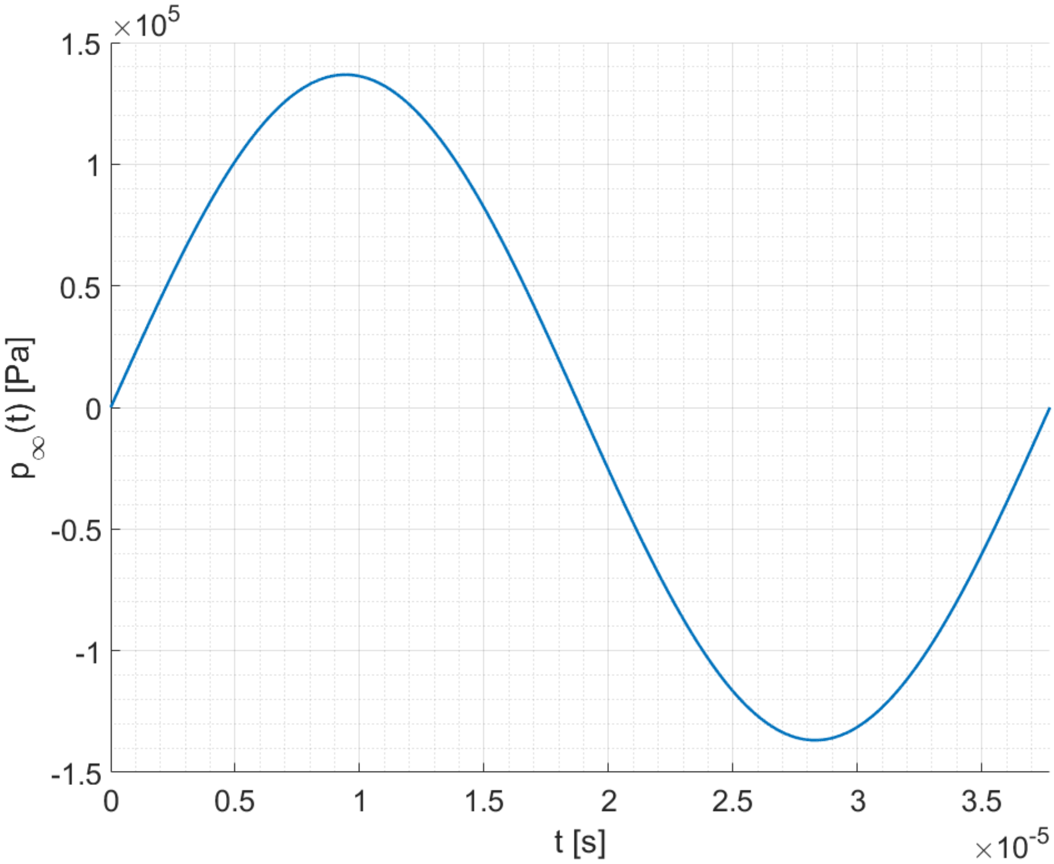

Figure 4.3: Driving sound waves

This graphic show a period of the driving sound wave described by the equation:

$$p_\infty(t) = P_A \sin(\omega t)$$

It is important to note that the behaviour of the bubble is strictly dependent on the pressure amplitude P_A. In fact, for amplitude under $1.1arm$, and for the initial conditions used, bubble collapse can not be seen [42].

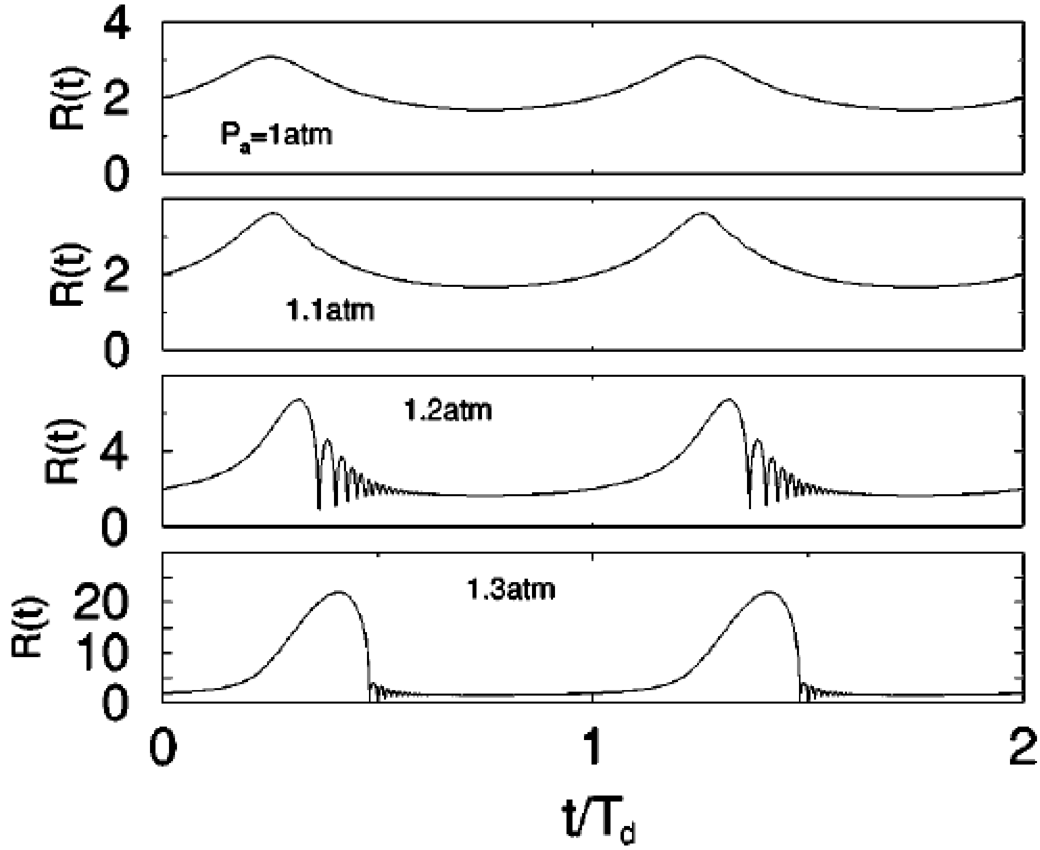

Figure 4.4: Radius evolution dependency on the pressure amplitude [42]

The next 3 plots show the dynamical behaviour of the interface.
The first one is just a typical solution of the RP equation for the radius. The second one is the radius in logarithmic scale for the y axis.
From this graphic one can easily see that the the maximum radius, during the expansion, differs from the minumum radius, obtained during the collapse, of 2 order of magnitude.
The third plot is a representation of the interface velocity $\dot{R}$. What can be see from this one is the high (negative) velocity that the bubble reaches during the collapse. During the 90s this result was at the base of the research of a model that include shock wave.

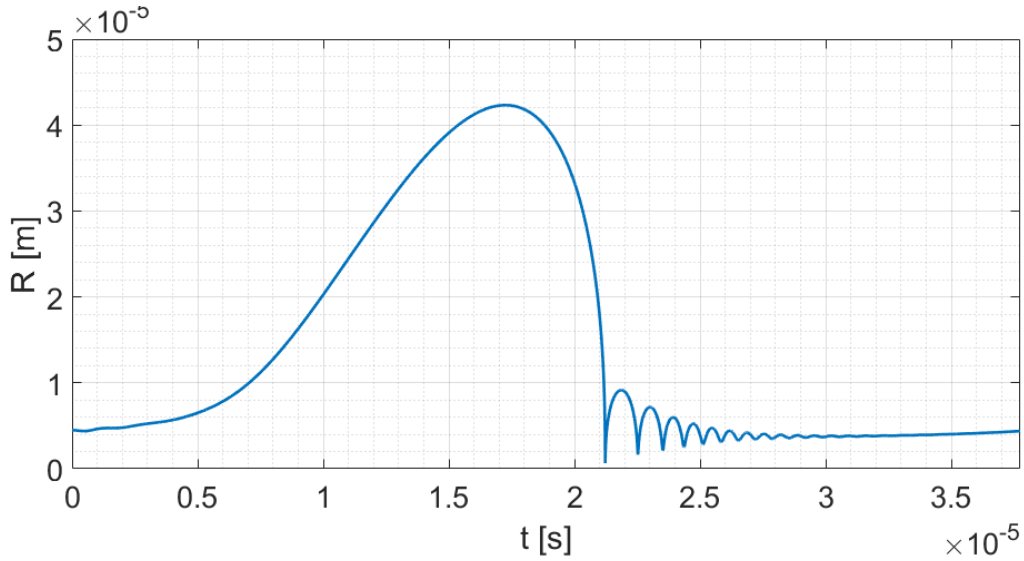

Figure 4.5: Bubble radius evolution

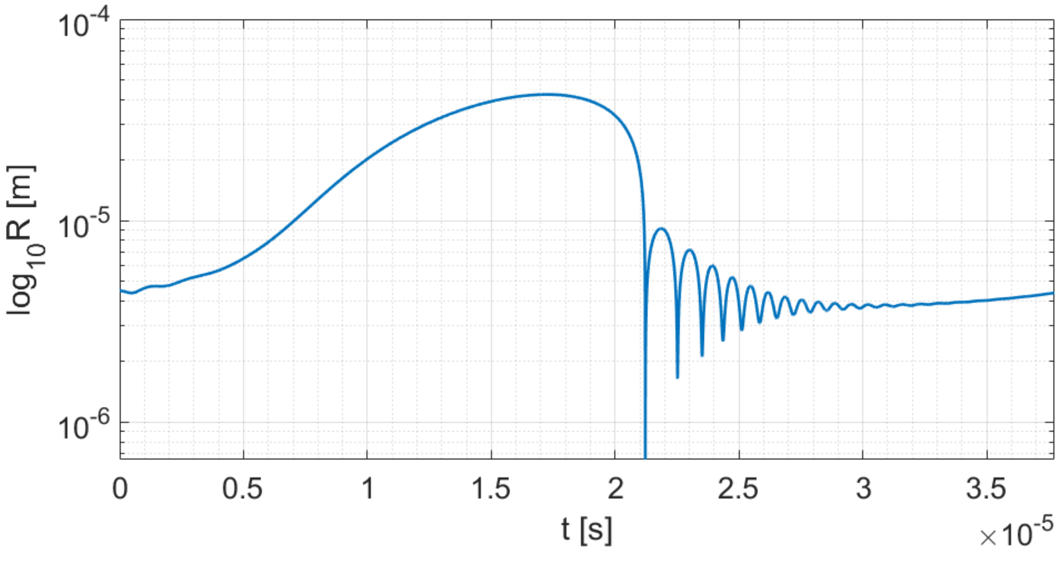

Figure 4.6: Bubble radius evolution with logarithmic scale for y axis

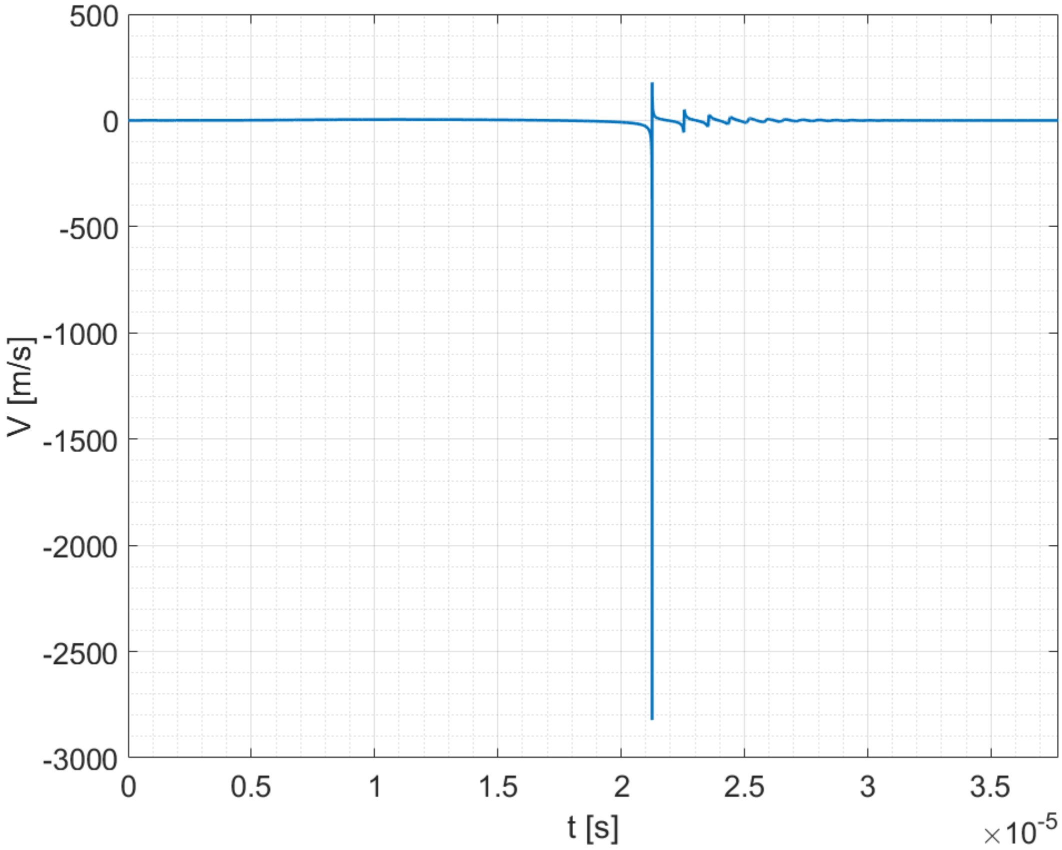

Figure 4.7: Bubble wall velocity

The most important parameters talking about sonoluminescence are without any doubt the temperature and the pressure inside the bubble.
Using the van der Waals relation cited at the beginning of this section, the numerical analysis have supplied a peak of pressure and a peak of temperature respectively of:

$$P_{G_{max}} = 5.792e + 09Pa$$

$$T_{G_{max}} = 2.398e + 04K$$

These results agree perfectly with the data obtained by Hiller and Putterman with the analysis of the spectrum [26].

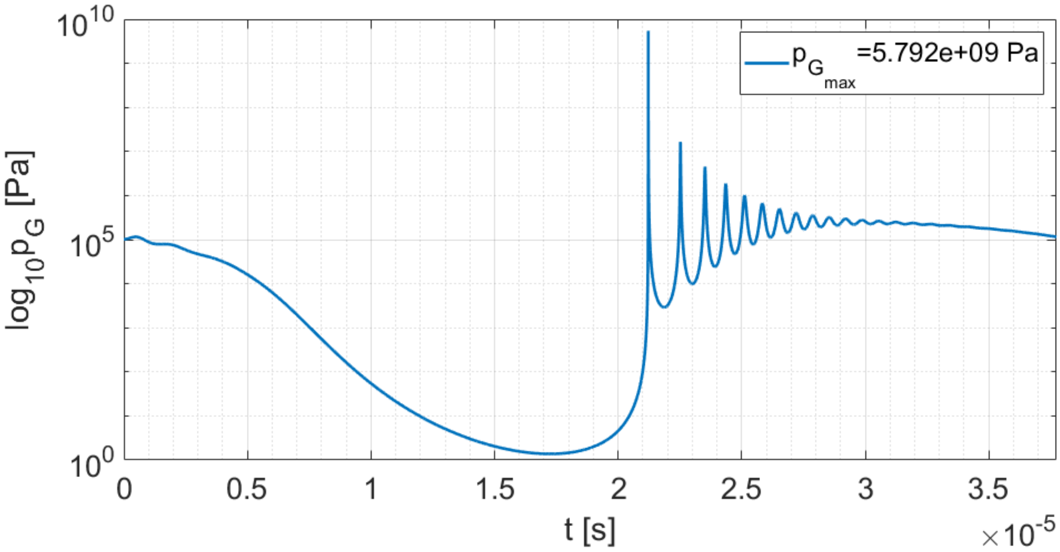

Figure 4.8: Pressure inside the bubble with logarithmic scale for y axis

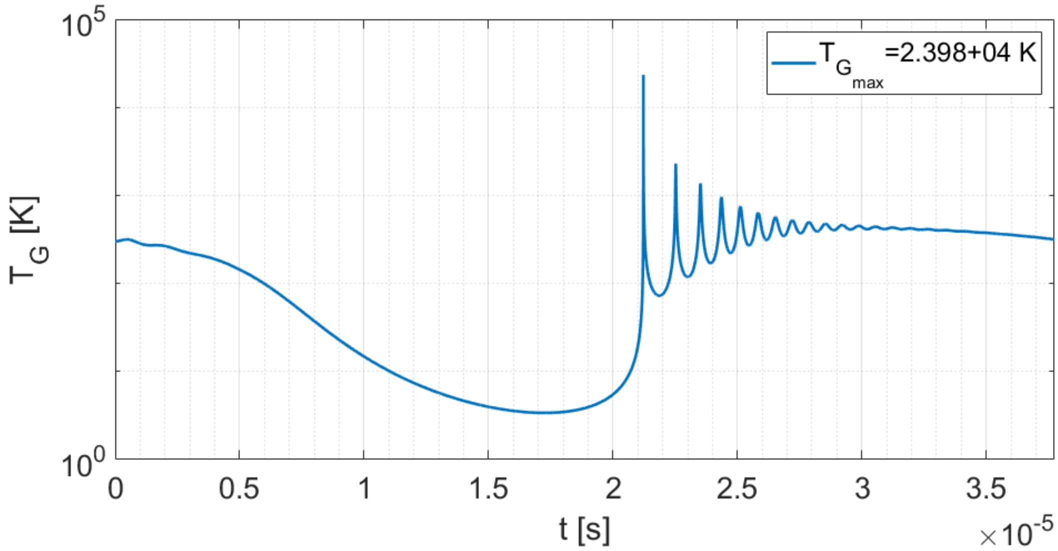

Figure 4.9: Pressure inside the bubble with logarithmic scale for y axis

4.1 Comparison between the physical and the analytical approach

This section is the core of the thesis. In the previous section, I have reproduced the numerical results obtained many times in the last 50 years, as a starting point for the following comparisons.

One can think to analyze the sequence of compressions of the bubble during a period by numerical interpolation through a spimplified version of the analytical solution demonstrated by Merle *et al.* in *On the implosion of a three dimensional compressible fluid* [52].

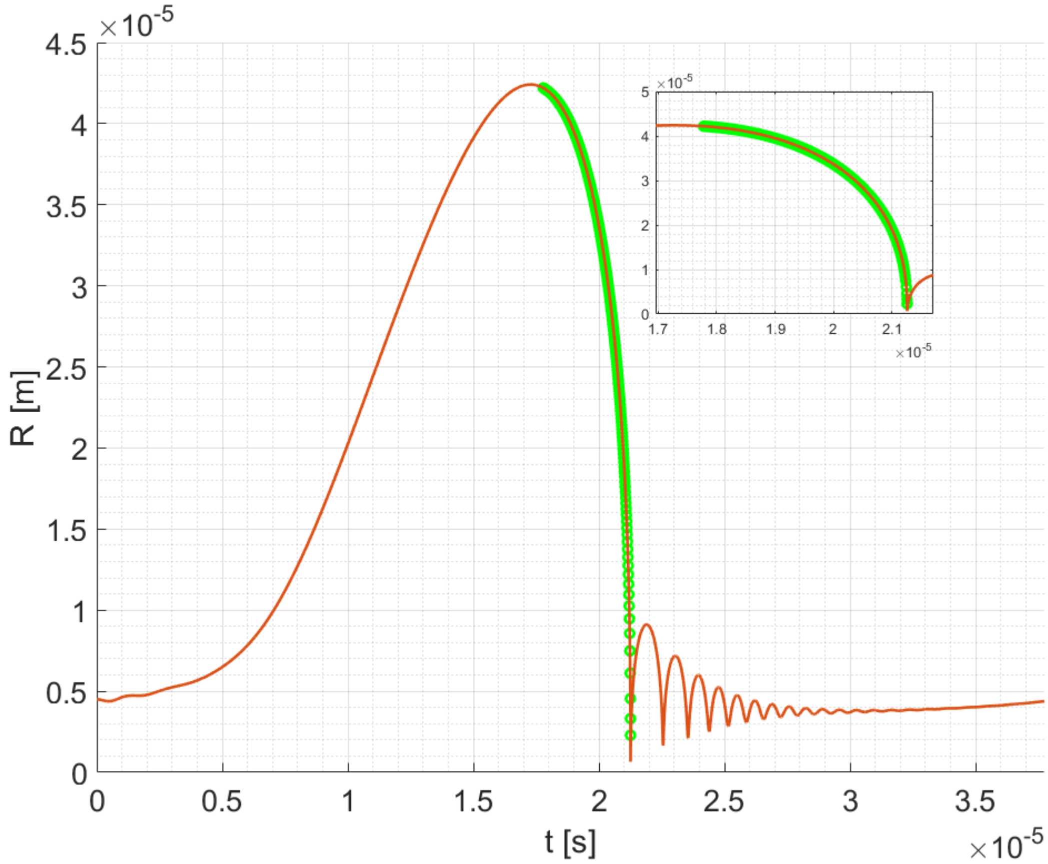

Figure 4.10: Points for radius interpolation for the first collapse

The first step of the analysis consists in the evaluation of the local minima and maxima of the radius numerical solution by the RP equation and the corresponding indexes with the matlab function:

$$[k_{min}, index_{min}] = min(\mathbf{solution})$$

$$[k_{max}, index_{max}] = max(\mathbf{solution})$$

This procedure must be done for every bounce reducing each time the vector of the solution to $\mathbf{solution}(index_{min} + 1 : end)$ where the value of $index_{min}$ is referred to the last bounce evaluated.

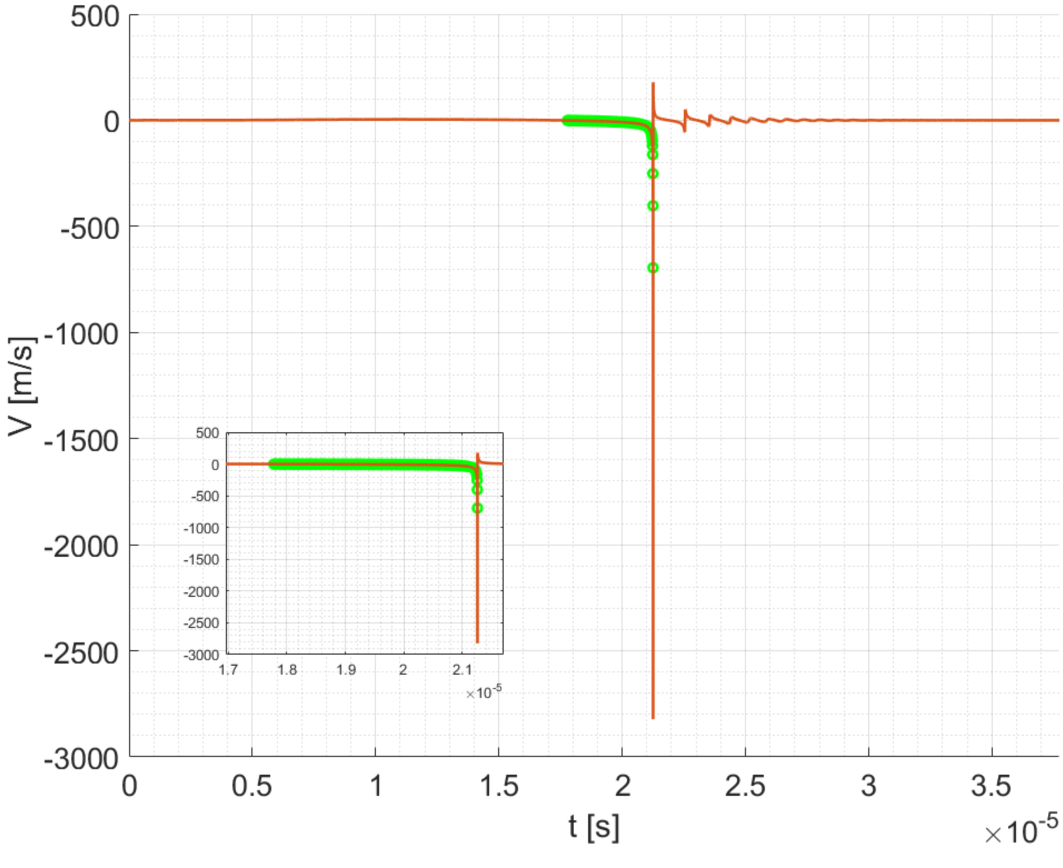

Figure 4.11: Points for velocity interpolation for the first collapse

One can observe that after the first three collapses it is possible to find local maxima and minima but the number of points between these two values reduces too much for a significant analysis.
The indexes obtained for the radius have been applied to vectors of data of velocity dR/dt.
Some data have been discarded from both the beginning and the end of the vectors because of the behaviour of the velocity that near the collapsing times it tends to blow up so rapidly in a time step so short that Matlab can not evaluate the derivatives.
In the figures from 4.10 to 4.15 are reported the plots of the data used in the next paragraph for the interpolations.

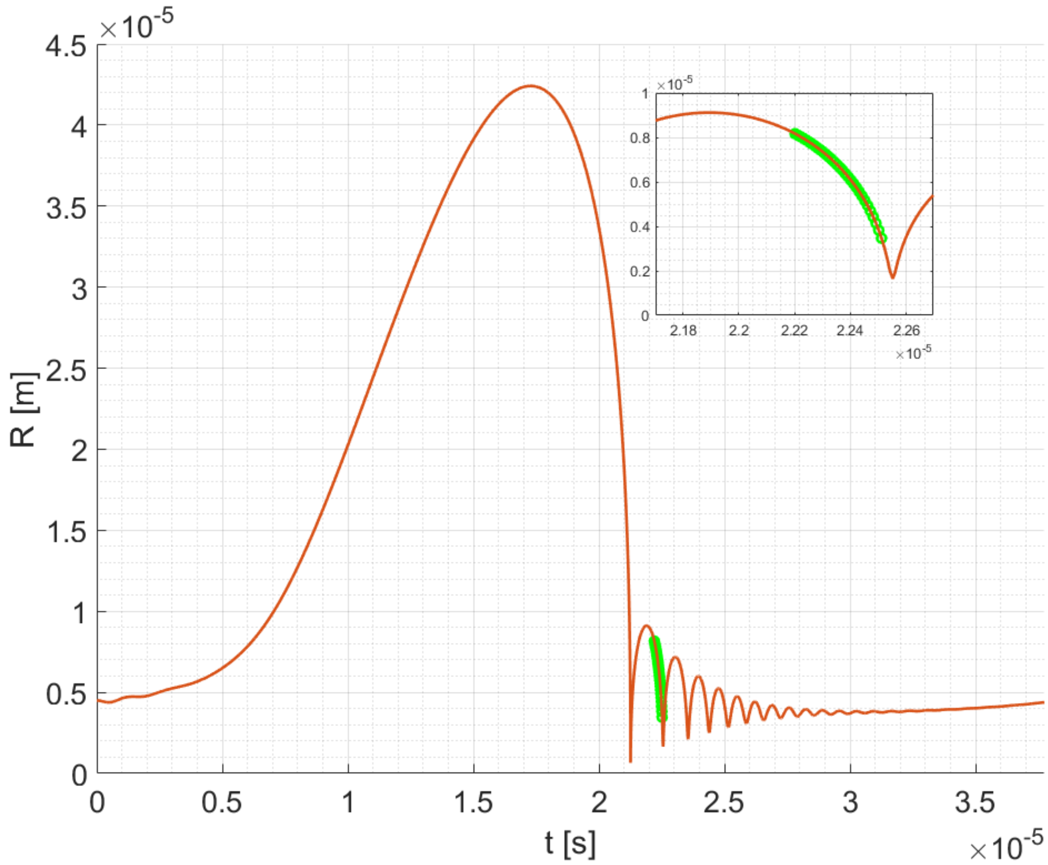

Figure 4.12: Points for radius interpolation for the second collapse

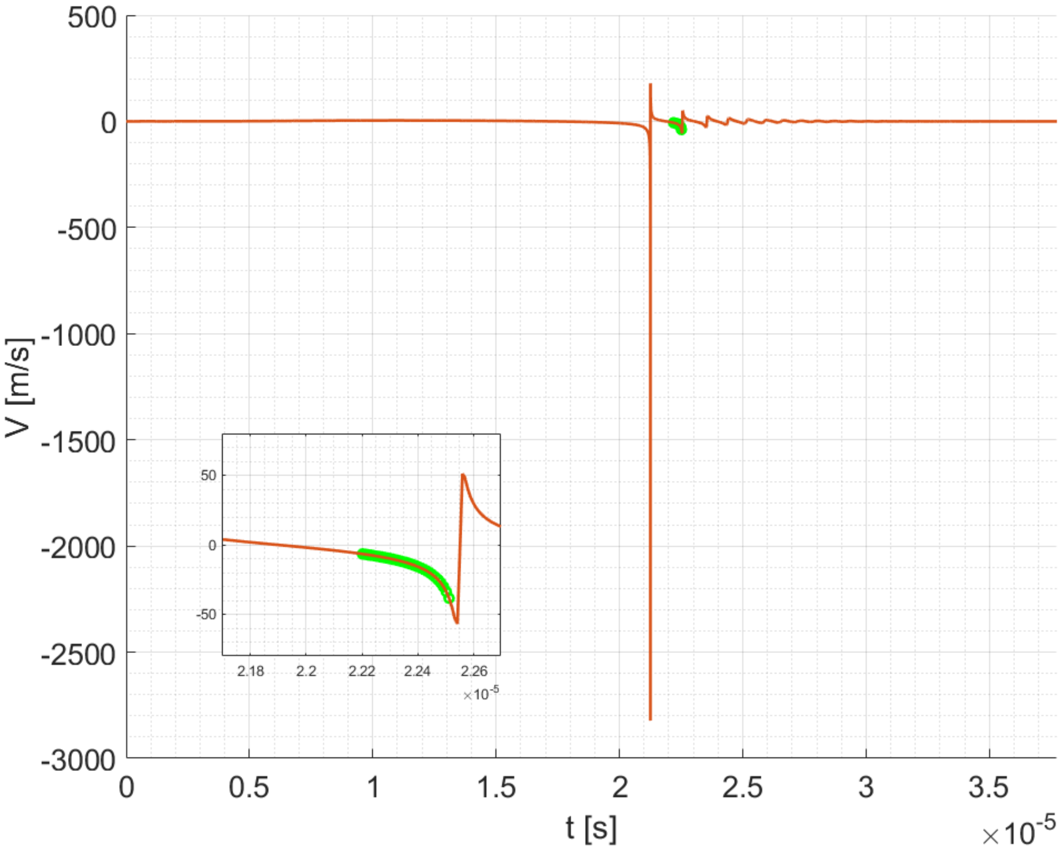

Figure 4.13: Points for velocity interpolation for the second collapse

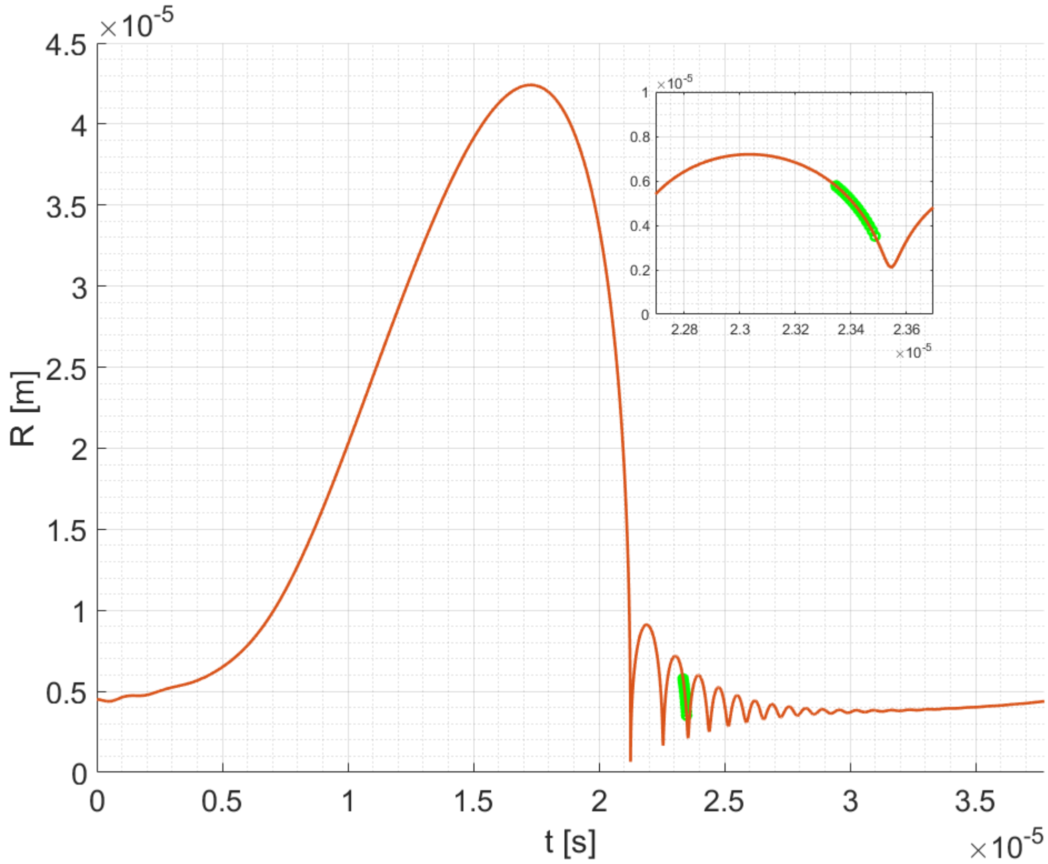

Figure 4.14: Points for radius interpolation for the third collapse

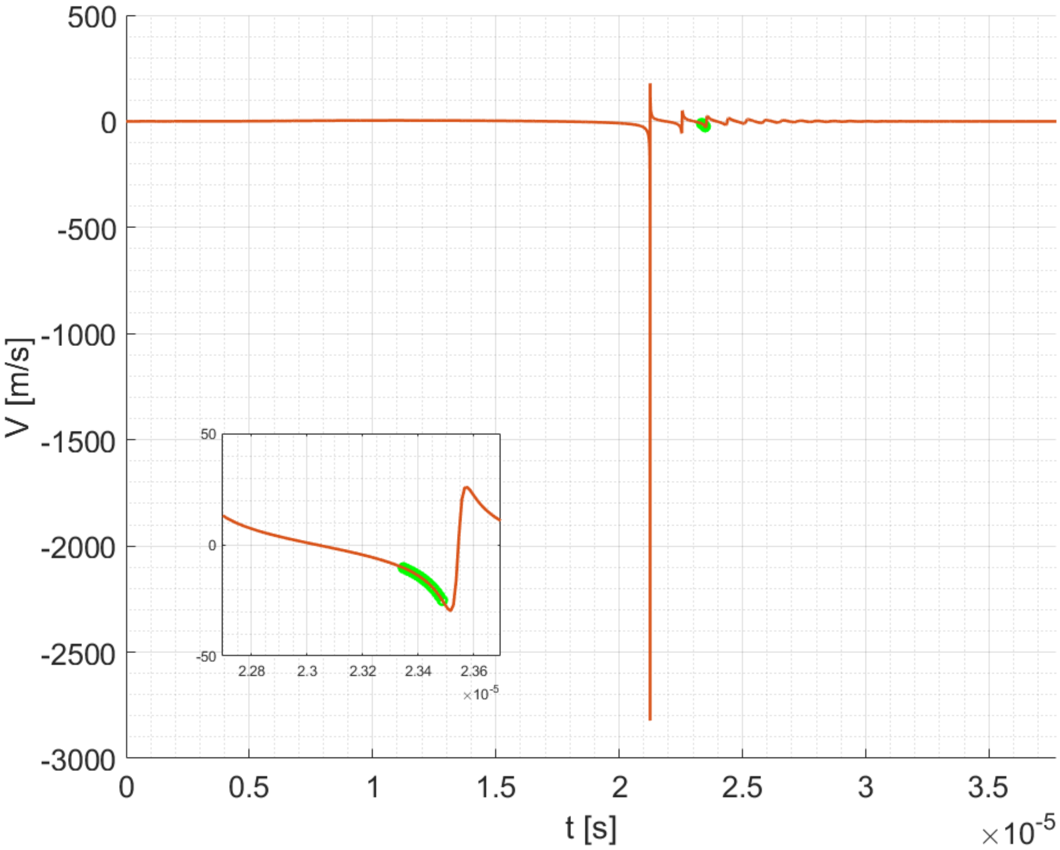

Figure 4.15: Points for velocity interpolation for the third collapse

4.1.1 Interpolation results

According to *On the implosion of a three dimensional compressible fluid* blow up profiles have the following structures [52]:

$$||u(t,\cdot)||_{L\infty} = \frac{c_{u0}(1+o_{t\to T}(1))}{(T-t)^{\frac{r_k-1}{r_k}}}$$

$$||\rho(t,\cdot)||_{L\infty} = \frac{c_{\rho 0}(1+o_{t\to T}(1))}{(T-t)^{\frac{l(r_k-1)}{r_k}}}$$

The function for the velocity profiles can be simplified in such way:

$$u(t) = \frac{c_{u0}}{(t_s-t)^{\frac{r_k-1}{r_k}}}$$

This function can be easily implemented in a software in order to fit different sets of data.
The interpolation is done with the MatLab tool *Curve Fitting Tool* (Matlab code reported in Appendix A) using the following custom function:

$$f(x) = \frac{a}{x^b}$$

Where $a = c_{u_0}$ and $b = \frac{r_k-1}{r_k}$ are free parameters, and the x and y vectors are respectively the corrected time $t_s - t$ and the velocity dR/dt.
The collapsing time t_s is referred in each case at the subsequent point of blow up of the first 3 oscillations that is defined as the point of local minimum found by:

$$t_s = t(k_{min})$$

where:

$$[k_{min}, index_{min}] = min(\textbf{solution})$$

This analysis produced the following results:

a_1	-0.002225 with 95% confidence bounds: $(-0.002403, -0.002047)$
a_2	-0.0001339 with 95% confidence bounds: $(-0.0001954, -7.243e-05)$
a_3	-0.002035 with 95% confidence bounds: $(-0.003586, -0.0004843)$
b_1	0.6182 with 95% confidence bounds: $(0.6141, 0.6223)$
b_2	0.7407 with 95% confidence bounds: $(0.7124, 0.769)$
b_3	0.5555 with 95% confidence bounds: $(0.5089, 0.6021)$

Table 4.3: Interpolation free parameters. Subscripts 1,2 and 3 represent the sequence of collapses

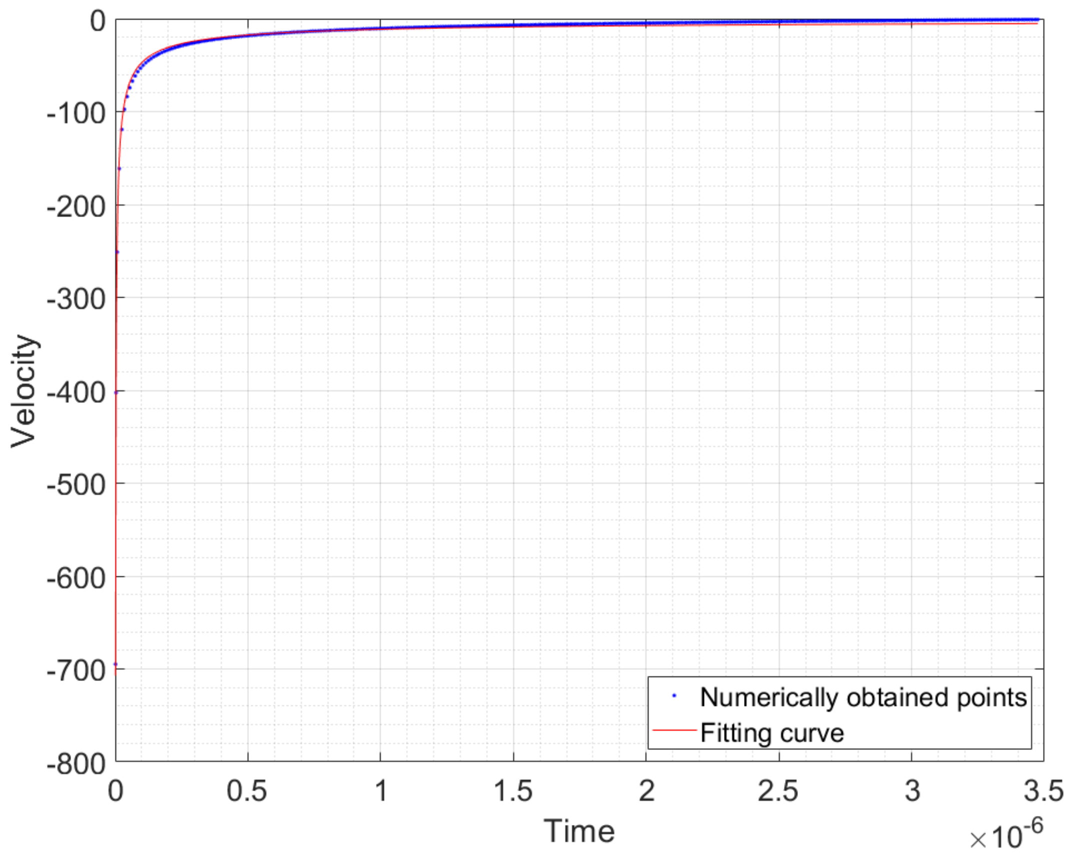

Figure 4.16: First bounce interpolation

From $b = \frac{r_k - 1}{r_k}$ it is possible to estimate 3 values of the discrete sequence of blow up speed $(r_k)_{k \geq 1}$:

$$r_k = -\frac{1}{b-1}$$

$r_k(b_1)$	2.6192
$r_k(b_2)$	3.8565
$r_k(b_3)$	2.2497

Table 4.4: Estimated values of the blow up speed sequence

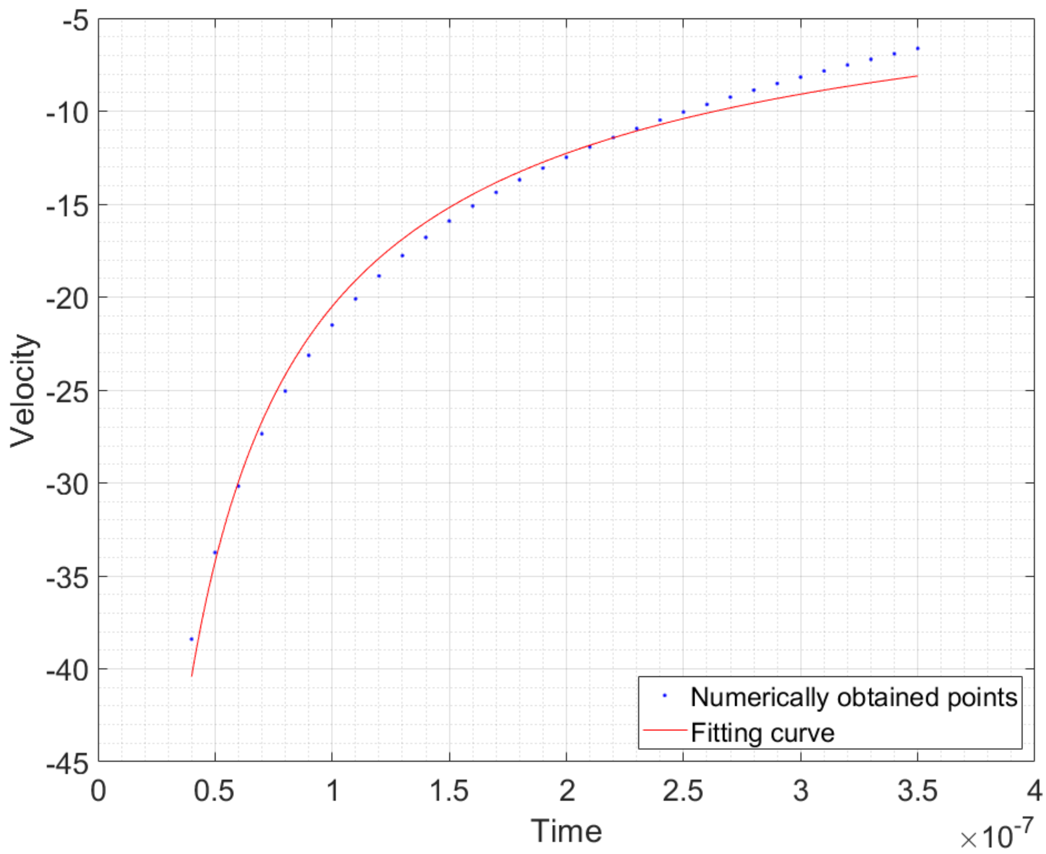

Figure 4.17: Second bounce interpolation

From the equation of density, knowing that for NS the parameter $l > \sqrt{3}$ one can assert that the lower bound of the exponent of the equation for ρ is:

$b_{1,\rho}$	1.0708
$b_{2,\rho}$	1.2829
$b_{3,\rho}$	0.9622

Table 4.5: Estimated lower bound for exponent of ρ

The figures from 4.16 to 4.18 show the curves obtained through the procedure discussed above.

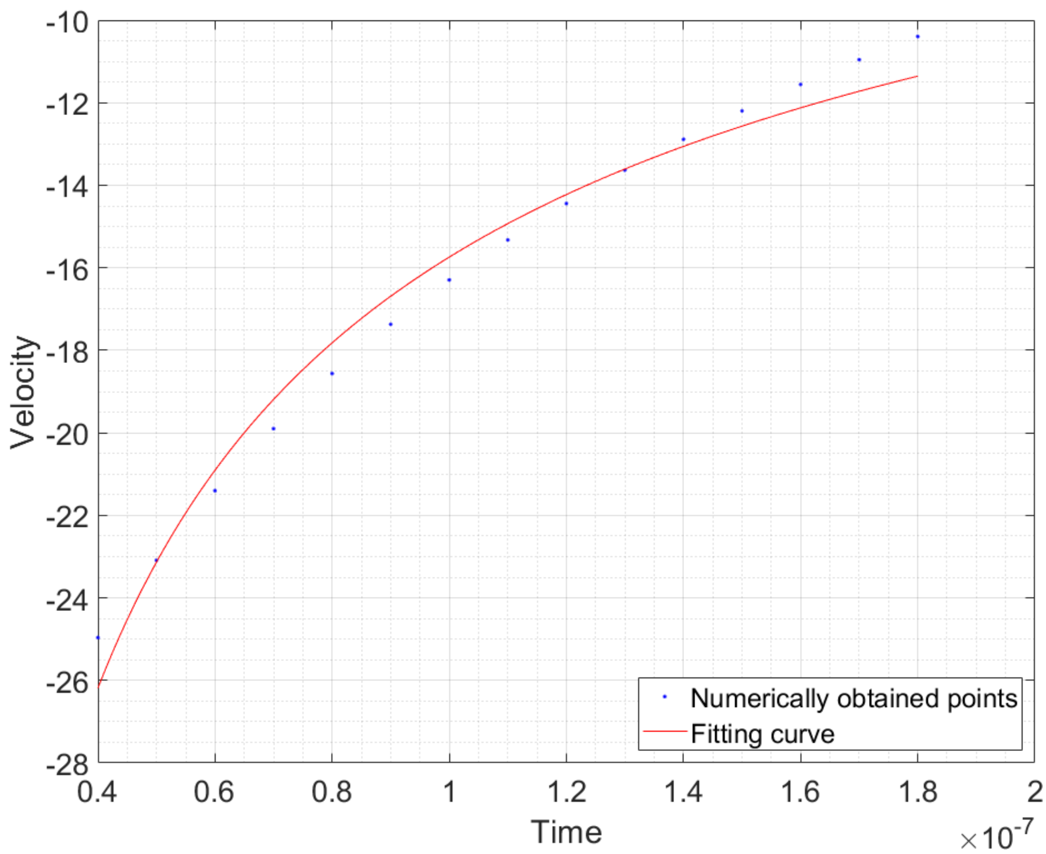

Figure 4.18: Third bounce interpolation

Chapter 5

Conclusions

In summary, in this work of master thesis I have carried out a preliminary analysis of the analytical solutions to the Navier-Stokes equation found by Merle *et al.* in a physical context in which they have not yet been taken into consideration.
Fitting the first three bounce of the numerical solution to the RP equation, I found three possible values of the discrete sequence of blow up speed (r_k) described in the theorem 1.1 of *On the implosion of a three dimensional compressible fluid* [52]. The numerical values obtained seem to be feasonable even compared with the exponent of the solution found by Guderley [6]. This reflects expectations, as the Guderley method was used for the construction of Euler's self-similar solutions by Merle *et al.* in the paper *On smooth self-similar solutions to the compressible Euler equations* [51].

Despite the number of points available for the interpolation of the second and the third collapse is very restricted, the coefficient found are in the neighborhood of the first one and so them can be considered acceptable.
Even if the solution considered is for the full compressible Navier-Stokes equations, it has been used just to evaluate collapsing profiles without taking into account neither that the fluid outside and the fluid inside the interface differ nor that the bubble doesn't explode.

The reason at the base of the possible link between these solutions and SBSL

is that both present a rapid growth of all the thermodynamic variables. What is called *strong singularity* in the works of Merle *et al.* could be at the base of the still today unknown mechanism of sonoluminesce.
Despite that, a combination of different chemical, physical and mathematical aspects is necessary for a full comprehension of this mechanism.

5.1 Future perspectives

Relatively to this work, a deeper study requires more computational power. It would be necessary to use a smaller fixed-step time interval (order of $10^{-18}s$) in order to refine the values obtained with the fitting and extend the analysis to the following bounces. In fact, after the third collapse the effects of viscosity start to come out and this make solutions smoother and this is what deteriorate a little bit the self-similarity of the solutions.

The RP model used in this work is very simple and another refinement could be to introduce a more complex version of the model inside the code and the latter can be coupled to a finer model for the interior dynamics.

Another possible development could be related to a DNS approach of the interior of the bubble coupling some model of chemical non-equilibrium and adding a refined model for condensation-evaporation, for example through the Raoult equation.

The interest around the sonoluminescing bubbles is not only related to the possible comprehension of the phenomenon but also on the possible capacity to use the great amount on energy focused in the center of the bubble for sonochemistry, ultrasound diagnostic, piezoacoustic inkjet printing, drag reduction and other applications [49].
For such reasons it should be studied more.

Appendix A

MatLab code

The main code is:

```
clc
close all

P_a = 1.35*101325;
R0 = 4.5e-6;
T0 = 300;
rho = 1000;
c = 1481; % Velocità del suono in acqua
k = 5/3;
a = R0/8.54;
p0 = 101325;
mu = 3e-3;
S = 3e-2;

out = sim('fun_simulink_6')

Temp_max = max(out.simout2);
p_max = max(out.simout3);

figure(1)
hold on
```

```
plot (out.tout,out.simout4,'linewidth',2);
grid on
grid minor
xlabel('t [s]')
ylabel('p_\infty(t)')
xlim ([0 out.tout(end)])

font_sz = 15;
x0=0; %definisco la dimensione del grafico con coordinate
y0=0;
width=1000;
height=500;
set(gcf,'position',[x0,y0,width,height])
set(gca, 'units', 'normalized'); %le seguenti 4 righe eliminano...
    i
%margini del grafico
Tight = get(gca, 'TightInset');
NewPos = [Tight(1)+0.05 Tight(2)+0.08 1-Tight(1)-Tight(3)-0.1 ...
    1-Tight(2)-Tight(4)-0.1];
set(gca, 'Position', NewPos);
set(gca,'fontsize',font_sz) %dimensione font

figure(2)
plot (out.tout,out.simout1,'linewidth',2);
hold on
grid on
grid minor
xlabel('t [s]')
ylabel('R [m]')
xlim ([0 out.tout(end)])

x0=0; %definisco la dimensione del grafico con coordinate
y0=0;
width=1000;
height=500;
set(gcf,'position',[x0,y0,width,height])
set(gca, 'units', 'normalized'); %le seguenti 4 righe eliminano...
    i
%margini del grafico
Tight = get(gca, 'TightInset');
```

```
NewPos = [Tight(1)+0.05 Tight(2)+0.08 1-Tight(1)-Tight(3)-0.1 ...
    1-Tight(2)-Tight(4)-0.1];
set(gca, 'Position', NewPos);
set(gca,'fontsize',font_sz) %dimensione font

figure(3)
semilogy (out.tout,out.simout1,'linewidth',2);
hold on
grid on
grid minor
xlabel('t [s]')
ylabel('log_{10}R [m]')
xlim ([0 out.tout(end)])

x0=0; %definisco la dimensione del grafico con coordinate
y0=0;
width=1000;
height=500;
set(gcf,'position',[x0,y0,width,height])
set(gca, 'units', 'normalized'); %le seguenti 4 righe eliminano...
    i
%margini del grafico
Tight = get(gca, 'TightInset');
NewPos = [Tight(1)+0.05 Tight(2)+0.08 1-Tight(1)-Tight(3)-0.1 ...
    1-Tight(2)-Tight(4)-0.1];
set(gca, 'Position', NewPos);
set(gca,'fontsize',font_sz) %dimensione font

figure(4)
plot (out.tout,out.simout,'linewidth',2);
hold on
grid on
grid minor
xlabel('t [s]')
ylabel('V [m/s]')
xlim ([0 out.tout(end)])

x0=0; %definisco la dimensione del grafico con coordinate
y0=0;
width=1000;
```

```
height=500;
set(gcf,'position',[x0,y0,width,height])
set(gca, 'units', 'normalized'); %le seguenti 4 righe eliminano...
    i
%margini del grafico
Tight = get(gca, 'TightInset');
NewPos = [Tight(1)+0.05 Tight(2)+0.08 1-Tight(1)-Tight(3)-0.1 ...
    1-Tight(2)-Tight(4)-0.1];
set(gca, 'Position', NewPos);
set(gca,'fontsize',font_sz) %dimensione font

figure(5)
semilogy (out.tout,out.simout2,'linewidth',2);
hold on
grid on
grid minor
xlabel('t [s]')
ylabel('T_G [K]')
xlim ([0 out.tout(end)])
legend('T_{G_{max}}=2.398+04 K')
hold off

x0=0; %definisco la dimensione del grafico con coordinate
y0=0;
width=1000;
height=500;
set(gcf,'position',[x0,y0,width,height])
set(gca, 'units', 'normalized'); %le seguenti 4 righe eliminano...
    i
%margini del grafico
Tight = get(gca, 'TightInset');
NewPos = [Tight(1)+0.05 Tight(2)+0.08 1-Tight(1)-Tight(3)-0.1 ...
    1-Tight(2)-Tight(4)-0.1];
set(gca, 'Position', NewPos);
set(gca,'fontsize',font_sz) %dimensione font

figure(6)
semilogy(out.tout,out.simout3,'linewidth',2);
hold on
grid on
```

```
grid minor
xlabel('t [s]')
ylabel('log_{10}p_G [Pa]')
xlim ([0 out.tout(end)])
legend('p_{G_{max}}=5.792e+09 Pa')
hold off

x0=0; %definisco la dimensione del grafico con coordinate
y0=0;
width=1000;
height=500;
set(gcf,'position',[x0,y0,width,height])
set(gca, 'units', 'normalized'); %le seguenti 4 righe eliminano...
    i
%margini del grafico
Tight = get(gca, 'TightInset');
NewPos = [Tight(1)+0.05 Tight(2)+0.08 1-Tight(1)-Tight(3)-0.1 ...
    1-Tight(2)-Tight(4)-0.1];
set(gca, 'Position', NewPos);
set(gca,'fontsize',font_sz) %dimensione font

[k, index] = min(out.simout);
[k2, index2] = max(out.simout1);
velocita = out.simout(index2+50:index-4);
raggio = out.simout1(index2+50:index-4);
tempo = out.tout(index2+50:index-4);
T = out.tout(index);
tempo_aggiornato = (T-tempo);

figure(7)
hold on
plot (tempo,velocita,'og','linewidth',2)
plot (out.tout,out.simout,'linewidth',2);
grid on
grid minor
xlabel('t [s]')
ylabel('V [m/s]')
xlim ([0 out.tout(end)])

x0=0; %definisco la dimensione del grafico con coordinate
```

```
y0=0;
width=1000;
height=500;
set(gcf,'position',[x0,y0,width,height])
set(gca, 'units', 'normalized'); %le seguenti 4 righe eliminano...
     i
%margini del grafico
Tight = get(gca, 'TightInset');
NewPos = [Tight(1)+0.05 Tight(2)+0.08 1-Tight(1)-Tight(3)-0.1 ...
    1-Tight(2)-Tight(4)-0.1];
set(gca, 'Position', NewPos);
set(gca,'fontsize',font_sz) %dimensione font

axes('position',[.20 .25 .25 .25])
box on
plot (tempo,velocita,'og','linewidth',2)
hold on
plot (out.tout(1700:2200),out.simout(1700:2200),'linewidth',2);
grid on
grid minor
ylim ([-3000 500])
xlim ([out.tout(1700) out.tout(2200)])

figure(8)
hold on
plot (tempo,raggio,'og','linewidth',2)
plot (out.tout,out.simout1,'linewidth',2);
grid on
grid minor
xlabel('t [s]')
ylabel('R [m]')
xlim ([0 out.tout(end)])

x0=0; %definisco la dimensione del grafico con coordinate
y0=0;
width=1000;
height=500;
set(gcf,'position',[x0,y0,width,height])
set(gca, 'units', 'normalized'); %le seguenti 4 righe eliminano...
     i
```

```
%margini del grafico
Tight = get(gca, 'TightInset');
NewPos = [Tight(1)+0.05 Tight(2)+0.08 1-Tight(1)-Tight(3)-0.1 ...
    1-Tight(2)-Tight(4)-0.1];
set(gca, 'Position', NewPos);
set(gca,'fontsize',font_sz) %dimensione font

axes('position',[.60 .65 .25 .25])
box on
plot (tempo,raggio,'og','linewidth',2)
hold on
plot (out.tout(1700:2200),out.simout1(1700:2200),'linewidth',2)...
    ;
grid on
grid minor
ylim ([0 5e-5])
xlim ([out.tout(1700) out.tout(2200)])

[k3, index3] = min(out.simout(2180:end));
[k4, index4] = max(out.simout1(2180:end));
velocita3 = out.simout(2180+index4+30:2180+index3-4);
raggio3 = out.simout1(2180+index4+30:2180+index3-4);
tempo3 = out.tout(2180+index4+30:2180+index3-4);
T3 = out.tout(2180+index3);
tempo_aggiornato3 = (T3-tempo3);

figure(9)
hold on
plot (tempo3,raggio3,'og','linewidth',2)
plot (out.tout,out.simout1,'linewidth',2);
grid on
grid minor
xlabel('t [s]')
ylabel('R [m]')
xlim ([0 out.tout(end)])

x0=0; %definisco la dimensione del grafico con coordinate
y0=0;
width=1000;
height=500;
```

```
set(gcf,'position',[x0,y0,width,height])
set(gca, 'units', 'normalized'); %le seguenti 4 righe eliminano...
    i
%margini del grafico
Tight = get(gca, 'TightInset');
NewPos = [Tight(1)+0.05 Tight(2)+0.08 1-Tight(1)-Tight(3)-0.1 ...
    1-Tight(2)-Tight(4)-0.1];
set(gca, 'Position', NewPos);
set(gca,'fontsize',font_sz) %dimensione font

axes('position',[.60 .65 .25 .25])
box on
plot (tempo3,raggio3,'og','linewidth',2)
hold on
plot (out.tout(2200:2300),out.simout1(2200:2300),'linewidth',2)...
    ;
grid on
grid minor
ylim ([0 1e-5])
xlim ([out.tout(2200) out.tout(2300)])

figure(10)
hold on
plot (tempo3,velocita3,'og','linewidth',2)
plot (out.tout,out.simout,'linewidth',2);
grid on
grid minor
xlabel('t [s]')
ylabel('V [m/s]')
xlim ([0 out.tout(end)])

x0=0; %definisco la dimensione del grafico con coordinate
y0=0;
width=1000;
height=500;
set(gcf,'position',[x0,y0,width,height])
set(gca, 'units', 'normalized'); %le seguenti 4 righe eliminano...
    i
%margini del grafico
Tight = get(gca, 'TightInset');
```

```
NewPos = [Tight(1)+0.05 Tight(2)+0.08 1-Tight(1)-Tight(3)-0.1 ...
    1-Tight(2)-Tight(4)-0.1];
set(gca, 'Position', NewPos);
set(gca,'fontsize',font_sz) %dimensione font

axes('position',[.20 .25 .25 .25])
box on
plot (tempo3,velocita3 ,'og','linewidth',2)
hold on
plot (out.tout(2200:2300),out.simout(2200:2300),'linewidth',2);
grid on
grid minor
ylim ([-80 80])
xlim ([out.tout(2200) out.tout(2300)])

[k5, index5] = min(out.simout(2310:end));
[k6, index6] = max(out.simout1(2310:end));
velocita5 = out.simout(2310+index6+30:2310+index5-4);
raggio5 = out.simout1(2310+index6+30:2310+index5-4);
tempo5 = out.tout(2310+index6+30:2310+index5-4);
T5 = out.tout(2310+index5);
tempo_aggiornato5 = (T5-tempo5);

figure(11)
hold on
plot (tempo5,raggio5 ,'og','linewidth',2)
plot (out.tout ,out.simout1 ,'linewidth',2);
grid on
grid minor
xlabel('t [s]')
ylabel('R [m]')
xlim ([0 out.tout(end)])

x0=0; %definisco la dimensione del grafico con coordinate
y0=0;
width=1000;
height=500;
set(gcf,'position',[x0,y0,width,height])
set(gca, 'units', 'normalized'); %le seguenti 4 righe eliminano...
    i
```

```
%margini del grafico
Tight = get(gca, 'TightInset');
NewPos = [Tight(1)+0.05 Tight(2)+0.08 1-Tight(1)-Tight(3)-0.1 ...
    1-Tight(2)-Tight(4)-0.1];
set(gca, 'Position', NewPos);
set(gca,'fontsize',font_sz) %dimensione font

axes('position',[.60 .65 .25 .25])
box on
plot (tempo5,raggio5,'og','linewidth',2)
hold on
plot (out.tout(2300:2400),out.simout1(2300:2400),'linewidth',2)...
    ;
grid on
grid minor
ylim ([0 1e-5])
xlim ([out.tout(2300) out.tout(2400)])

figure(12)
hold on
plot (tempo5,velocita5,'og','linewidth',2)
plot (out.tout,out.simout,'linewidth',2);
grid on
grid minor
xlabel('t [s]')
ylabel('V [m/s]')
xlim ([0 out.tout(end)])

x0=0; %definisco la dimensione del grafico con coordinate
y0=0;
width=1000;
height=500;
set(gcf,'position',[x0,y0,width,height])
set(gca, 'units', 'normalized'); %le seguenti 4 righe eliminano...
     i
%margini del grafico
Tight = get(gca, 'TightInset');
NewPos = [Tight(1)+0.05 Tight(2)+0.08 1-Tight(1)-Tight(3)-0.1 ...
    1-Tight(2)-Tight(4)-0.1];
set(gca, 'Position', NewPos);
```

```
set(gca,'fontsize',font_sz) %dimensione font

axes('position',[.20 .25 .25 .25])
box on
plot (tempo5,velocita5 ,'og','linewidth',2)
hold on
plot (out.tout(2300:2400),out.simout(2300:2400),'linewidth',2);
grid on
grid minor
ylim ([-50 50])
xlim ([out.tout(2300) out.tout(2400)])


fit1(tempo_aggiornato, velocita)

fit2(tempo_aggiornato3, velocita3)

fit3(tempo_aggiornato5, velocita5)
```

The MatLab functions associated with the Simulink model `fun_simulink_6.slx...` are respectively:

- Rayleigh-Plesset function:

```
function R_dotdot = fcn(R_dot,R,p_a,p_a_dot,P_G,P_G_dot...
)

R0 = 4.5e-6;
rho = 1000;
c = 1481;
p0 = 101325;
mu = 3e-3;
S = 3e-2;

R_dotdot = -3/2*(R_dot^2/R)+P_G/(rho*R)-p0/(rho*R)+p_a...
/(rho*R)+1/(rho*c)*P_G_dot-4*mu*R_dot/(rho*R^2)-2*S/(rho...
*R^2);

```

- Pressure inside the bubble:

```
function P_G = fcn(R)

k = 5/3;
R0 = 4.5e-6;
P0 = 101325;
a = R0/8.54;

P_G = (P0*R0^(3*k))/(R^3-a^3)^k;
```

- Temperature inside the bubble:

```
function T_G = fcn(R)

R0 = 4.5e-6;
T0 = 300;
k = 5/3;
a = R0/8.54;

T_G = (T0*R0^(3*(k-1)))/(R^3-a^3)^(k-1);
```

- Driving sound wave:

```
function p_a = fcn(t)

p = 1.35;
P_a = 101325*p;
f = 26500;
w = 2*pi*f;

p_a = P_a*sin(w*t);
```

- Fit 1:

```
%% Fit: 'fit_1'.
[xData, yData] = prepareCurveData( tempo_aggiornato, ...
    velocita );

% Set up fittype and options.
ft = fittype( 'a/(x)^b', 'independent', 'x', 'dependent', '...
    y' );
opts = fitoptions( 'Method', 'NonlinearLeastSquares' );
```

```
opts.Display = 'Off';
opts.StartPoint = [0.0971317812358475 0.823457828327293];

% Fit model to data.
[fitresult, gof] = fit( xData, yData, ft, opts );

% Plot fit with data.
figure( 13 );
h = plot( fitresult, xData, yData);
legend( h, 'Numerically obtained points', 'Fitting curve', ...
    'Location', 'Southeast', 'Interpreter', 'none' );
% Label axes
xlabel( 'Time', 'Interpreter', 'none' );
ylabel( 'Velocity', 'Interpreter', 'none' );
grid on
grid minor

font_sz=20;
x0=0; %definisco la dimensione del grafico con coordinate
y0=0;
width=1000;
height=800;
set(gcf,'position',[x0,y0,width,height])
set(gca, 'units', 'normalized'); %le seguenti 4 righe ...
    eliminano i
%margini del grafico
Tight = get(gca, 'TightInset');
NewPos = [Tight(1)+0.05 Tight(2)+0.08 1-Tight(1)-Tight(3)-0...
    .1 1-Tight(2)-Tight(4)-0.1];
set(gca, 'Position', NewPos);
set(gca,'fontsize',font_sz) %dimensione font
```

- Fit 2:

```
%% Fit: 'fit_2'.
[xData, yData] = prepareCurveData( tempo_aggiornato3, ...
    velocita3 );
```

```

% Set up fittype and options.
ft = fittype( 'a/(x)^b', 'independent', 'x', 'dependent', '...
    y' );
opts = fitoptions( 'Method', 'NonlinearLeastSquares' );
opts.Display = 'Off';
opts.StartPoint = [0.890903252535798 0.959291425205444];

% Fit model to data.
[fitresult, gof] = fit( xData, yData, ft, opts );

% Plot fit with data.
figure( 14 );
h = plot( fitresult, xData, yData );
legend( h, 'Numerically obtained points', 'Fitting curve', ...
    'Location', 'Southeast', 'Interpreter', 'none' );
% Label axes
xlabel( 'Time', 'Interpreter', 'none' );
ylabel( 'Velocity', 'Interpreter', 'none' );
grid on
grid minor

font_sz=20;
x0=0; %definisco la dimensione del grafico con coordinate
y0=0;
width=1000;
height=800;
set(gcf,'position',[x0,y0,width,height])
set(gca, 'units', 'normalized'); %le seguenti 4 righe ...
    eliminano i
%margini del grafico
Tight = get(gca, 'TightInset');
NewPos = [Tight(1)+0.05 Tight(2)+0.08 1-Tight(1)-Tight(3)-0...
    .1 1-Tight(2)-Tight(4)-0.1];
set(gca, 'Position', NewPos);
set(gca,'fontsize',font_sz) %dimensione font
```

- Fit 3:

```
%% Fit: 'fit_2'.
[xData, yData] = prepareCurveData( tempo_aggiornato5, ...
    velocita5 );

% Set up fittype and options.
ft = fittype( 'a/(x)^b', 'independent', 'x', 'dependent', '...
    y' );
opts = fitoptions( 'Method', 'NonlinearLeastSquares' );
opts.Display = 'Off';
opts.MaxIter = 4000;
opts.StartPoint = [0.337719409821377 0.900053846417662];

% Fit model to data.
[fitresult, gof] = fit( xData, yData, ft, opts );

% Plot fit with data.
figure( 15 );
h = plot( fitresult, xData, yData );
legend( h, 'Numerically obtained points', 'Fitting curve', ...
    'Location', 'southeast', 'Interpreter', 'none' );
% Label axes
xlabel( 'Time', 'Interpreter', 'none' );
ylabel( 'Velocity', 'Interpreter', 'none' );
grid on
grid minor

font_sz=20;
x0=0; %definisco la dimensione del grafico con coordinate
y0=0;
width=1000;
height=800;
set(gcf,'position',[x0,y0,width,height])
set(gca, 'units', 'normalized'); %le seguenti 4 righe ...
    eliminano i
%margini del grafico
Tight = get(gca, 'TightInset');
NewPos = [Tight(1)+0.05 Tight(2)+0.08 1-Tight(1)-Tight(3)-0...
    .1 1-Tight(2)-Tight(4)-0.1];
```

```
set(gca, 'Position', NewPos);
set(gca,'fontsize',font_sz) %dimensione font
```

Appendix B

Bubbles in nature and art

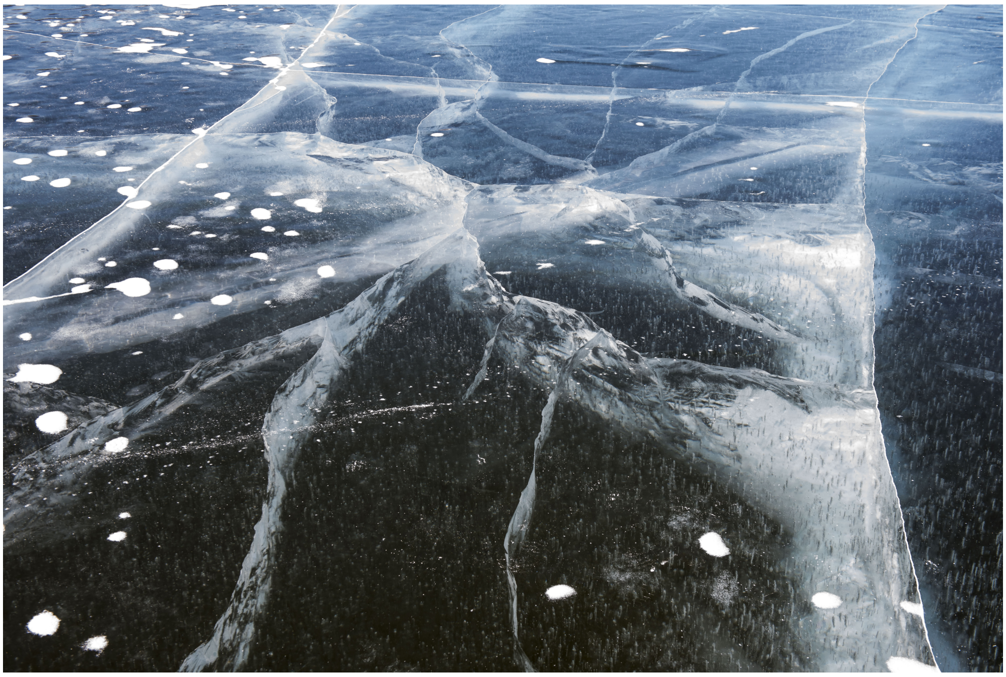

Figure B.1: Air bubbles in the ice on Baikal Lake (Russia, 2018), courtesy of Raffaella Canfarini [53]

Figure B.2: Air bubbles in the ice on Baikal Lake (Russia, 2018), courtesy of Raffaella Canfarini [53]

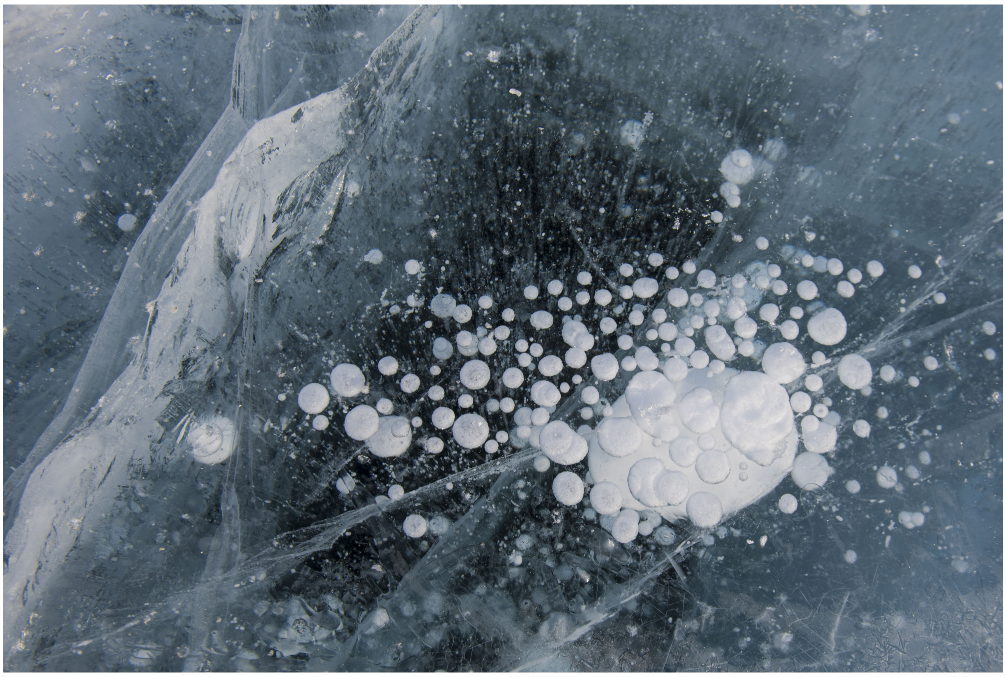

Figure B.3: Air bubbles in the ice on Baikal Lake (Russia, 2018), courtesy of Raffaella Canfarini [53]

Figure B.4: Air bubbles in the ice on Baikal Lake (Russia, 2018), courtesy of Raffaella Canfarini [53]

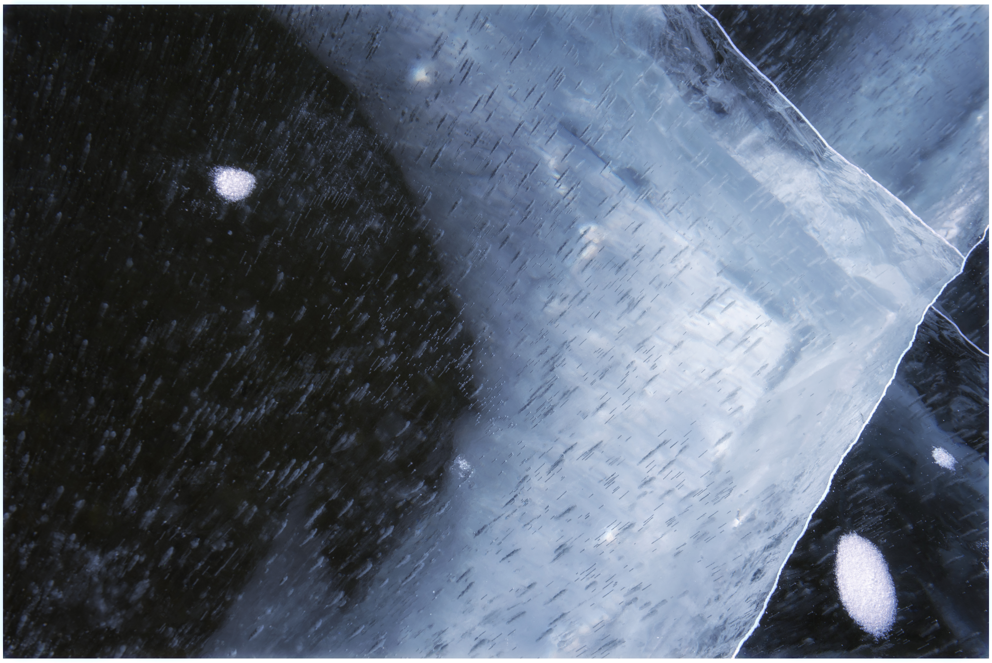

Figure B.5: Air bubbles in the ice on Baikal Lake (Russia, 2018), courtesy of Raffaella Canfarini [53]

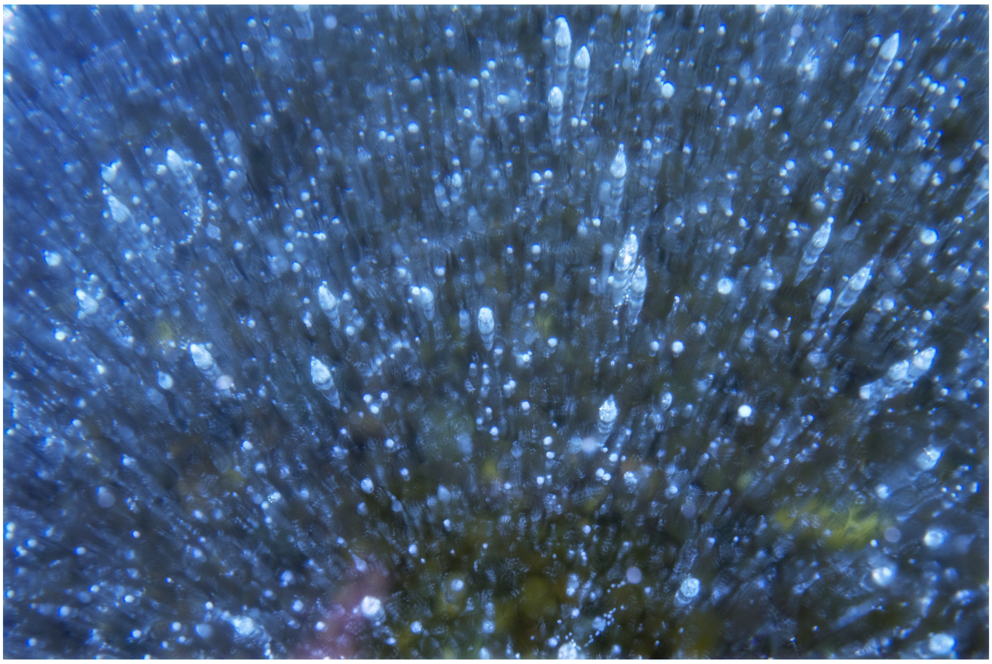

Figure B.6: Air bubbles in the ice on Baikal Lake (Russia, 2018), courtesy of Raffaella Canfarini [53]

Figure B.7: Glass bubbles in a fountain (Verona, 2019), courtesy of Raffaella Canfarini [53]

Figure B.8: Glass bubbles in a fountain (Verona, 2019), courtesy of Raffaella Canfarini [53]

Figure B.9: Resin bubble on Pinus radiata tree stump (16 December 2007), Tony Wills [54]

Bibliography

[1] Besant W.H. «Hydrostatics and hydrodynamics». In: *Cambridge University Press* (1859) (cit. on p. 4).

[2] Thornycroft J.I. and Walker S.W. «Torpedo-boat destroyers». In: *Minutes of the Proceedings of the Institution of Civil Engineers* 122 (1895), pp. 51–69 (cit. on p. 4).

[3] Lord Rayleigh. «On the pressure developed in a liquid on the collapse of a spherical cavity». In: *Philos. Mag.* 34 (1917), p. 94 (cit. on pp. 4, 10).

[4] Marinesco N. and Trillat J.J. «Action des ultrasons sur les plaques photographiques». In: *Proc. R. Acad. Sci. Amsterdam* 196 (1933), pp. 858–860 (cit. on p. 5).

[5] Frenzel H. and Schultes H. «Lumineszenz im ultraschall-beschickten Wasser». In: *Z. Phys. Chem. Abt. B* 27B, (1934), pp. 421–424 (cit. on p. 5).

[6] Guderley G. «Starke kugelige und zylindrische Verdichtungsstosse in der Nahe des Kugelmittelpunktes bzw. der Zylinderachse». In: *Luftahrtforschung* 19 (1942), p. 302 (cit. on pp. 17, 20, 46).

[7] Plesset Milton. «The dynamics of Cavitation Bubbles». In: *J. Appl. Mech.* 16 (1949), p. 277 (cit. on pp. 4, 10–12).

[8] Noltingk B. and Neppiras E. «Cavitation Produced by Ultrasonics». In: *Proceedings of the Physical Society* 63 (1950), pp. 674–685 (cit. on p. 5).

[9] Gilmore F.R. «The growth or collapse of a spherical bubble in a viscous compressible liquid». In: *Calif. Inst. of Tech. Hydrodynamics Lab. Rep.* 26-4 (1952) (cit. on pp. 5, 14).

[10] Poritsky H. «The collapse or growth of a spherical bubble or cavity in a viscous fluid». In: *Proc. First Nat. Cong. in Appl. Mech.* (1952), pp. 813–821 (cit. on p. 5).

[11] Plesset Milton. «On the stability of fluid flows with spherical symmetry». In: *J. Appl. Phys.* 25 (1954), p. 96 (cit. on p. 5).

[12] Plesset Milton and T. P. Mitchell. «On the stability of the spherical shape of a vapor cavity in a liquid». In: *Q. Appl. Math.* 13 (1956), pp. 419–430 (cit. on p. 5).

[13] Lauterborn W. «Numerical investigation of nonlinear oscillations of gas bubbles in liquids». In: *J. Acoust. Soc. Am.* 59 (1976), p. 283 (cit. on pp. 5, 10).

[14] Plesset Milton and Prosperetti Andrea. «Bubble Dynamics and cavitation». In: *Ann. Rev. Fluid Mech* 9 (1977), pp. 145–185 (cit. on pp. 5, 10).

[15] Tomita Y. and Shima A. «On the behavior of a spherical bubble and the impulse pressure in a viscous compressible liquid». In: *Bulletin of the JSME* (1977), 20-149 : 1453–1460 (cit. on p. 5).

[16] Shima A. and Tomita Y. «The behavior of a spherical bubble in mercury». In: *Rep. Inst. High Speed Mech.* 39 (1979), pp. 19–45 (cit. on p. 5).

[17] Shima A. and Fujiwara T. «The collapse of bubbles in compressible hydraulic oils,» in: *J. Acoust. Soc. Am.* 68 (1980), pp. 1509–1515 (cit. on p. 5).

[18] Keller J.B. and Miksis M. «Bubble oscillations of large amplitude». In: *J. Acoust. Soc. Am.* 68 (1980), pp. 628–633 (cit. on p. 14).

[19] Landau L.D. and Lifshitz E.M. *Fluid Mechanics.* Ed. by Butterworth-Heinemann. 1987 (cit. on pp. 7, 16).

[20] Bird R.B., Armstrong R.C., and Hassager O. *Dynamics of Polymeric Fluids: Volume 1 Fluid Mechanics.* Ed. by Wiley. 1987 (cit. on p. 9).

[21] Gaitan D.F. «Ph.D Thesis (The University of Mississipi». In: (1990) (cit. on p. 5).

[22] Gaitan D.F. and Crum L.A. «Frontiers of Nonlinear Acoustics». In: *edited by M. F. Hamilton and D. T. Blackstock (Elsevier Appl. Sci, London)* (1990), pp. 459–463 (cit. on p. 5).

[23] Barber B.P. and Putterman S. «Observation of synchronous picosecond sonoluminescence». In: *Nature* 352 (1991), pp. 318–320 (cit. on p. 5).

[24] Barber B.P., Hiller R., Arisaka K., Fetterman H., and Putterman S. «Resolving the picosecond characteristics of synchronous sonoluminescence». In: *J. Acoust. Soc. Am.* 91 (1992), pp. 3061–3063 (cit. on p. 5).

[25] Gaitan D.F., Crum L.A., and Roy R.A. «Sonoluminescence and bubble dynamics for a single, stable, cavitation bubble». In: *J. Acoust. Soc. Am.* 91 (1992), pp. 3166–3183 (cit. on p. 5).

[26] Hiller R. and Putterman S.J. «Spectrum of synchronous picosecond sonoluminescence». In: *Phys. Rev. Lett.* 69 (1992), pp. 1182–1184 (cit. on p. 34).

[27] Wu C.C. and Roberts P.H. «Shock-wave propagation in a sonoluminescing gas bubble». In: *Phys. Rev. Lett.* 70 (1993), pp. 3424–3427 (cit. on p. 17).

[28] Greenspan H.P. and Nadim A. «On sonoluminescence of an oscillating gas bubble». In: *Phys. Fluid A* 5 (1993), pp. 1065–1067 (cit. on p. 5).

[29] Löfstedt R., Barber B.P., and Putterman S.J. «Toward a hydrodynamic theory of sonoluminescence». In: *Phys. Fluids A* 5 (1993), pp. 2911–2928 (cit. on pp. 17, 29, 30).

[30] Frommhold L. and Atchley A.A. «Is sonoluminescence due to collision-induced emission?» In: *Phys. Rev. E* 73 (1994), pp. 2883–2886 (cit. on p. 5).

[31] Brenner M.P., Hilgenfeldt S., and T.F. Dupont. «Bubble Shape Oscillations and the Onset of Sonoluminescence». In: *Phys. Rev. Lett* 75 (1995), p. 954 (cit. on p. 5).

[32] Garcia N. and Levanyuk A.P. «Sonoluminescence: a new electrical breakdown hypothesis». In: *Pis'ma Zh. Eksp. Teor. Fiz* 64 (1996), pp. 849–852 (cit. on p. 5).

[33] Hilgenfeldt S., Lhose D., and Brenner M.P. «Phase diagrams for sonoluminescing bubbles». In: *Phys. Fluids* 8 (1996), p. 2808 (cit. on p. 5).

[34] Vuong V.Q. and Szeri A.J. «Sonoluminescence and diffusive transport». In: *Phys. Fluids* 8 (1996), pp. 2354–2364 (cit. on p. 17).

[35] Prosperetti A. «A new mechanism for sonoluminescence». In: *J. Acoust. Soc. Am.* 101 (1997), pp. 2003–2007 (cit. on p. 5).

[36] Barber Bradley P., Hiller Robert A., Löfstedt Ritva, Putterman Seth J., and Weninger Keith R. «Defining the unknowns of sonoluminescence». In: *Physics Reports* 281 (1997), pp. 65–143 (cit. on p. 16).

[37] Moss W.C. «Understanding the periodic driving pressure in the Rayleigh-Plesset equation». In: *J. Acoust. Soc. Am* 101 (1997), pp. 1187–1190 (cit. on p. 5).

[38] Cheng H.Y., Chu M.C., Leung P.T., and Yuan L. «How important are shock waves to single-bubble sonoluminescence?» In: *Phys. Rev. E* 58 (1998), pp. 2705–2708 (cit. on p. 17).

[39] Storey B.D. and Szeri A.J. «Water vapour, sonoluminescence and sonochemistry». In: *Proc. R. Soc. London, Ser. A* 456 (2000), pp. 1685–1709 (cit. on pp. 17, 18).

[40] Pope Stephen B. *Turbulent Flows*. Ed. by Cambridge University Press. 2000 (cit. on p. 7).

[41] Lin H. and Szeri A.J. «Shock formation in the presence of entropy gradients». In: *J. Fluid Mech* 431 (2001), pp. 161–188 (cit. on p. 17).

[42] Brenner Michael P., Hilgenfeldt Sascha, and Lohse Detlef. «Single-bubble sonoluminescence». In: *Reviews of modern physics* 74 (2002), pp. 426–472 (cit. on pp. 5, 14, 16, 17, 31, 32).

[43] Bird R.B., Stewart W.E., and Lightfoot E.N. *Transport Phenomena, 2^{nd} edition*. Ed. by Wiley. 2002 (cit. on p. 9).

[44] Prosperetti Andrea. «Bubbles». In: *Phys. Fluids* 16 (2004), p. 1852 (cit. on p. 1).

[45] Brennen Christopher E. «Bubble Growth and Collapse». In: *Cambridge University Press* (2005), pp. 73–96 (cit. on pp. 10, 14, 15).

[46] Behroozi F. «Soap bubbles in paintings: Art and science». In: *Am. J. Phys.* 76 (2008), p. 1087 (cit. on p. 1).

[47] Lauterborn W. and Kurz T. «Physics of bubble osclillations». In: *Rep. Prog. Phys.* 73 (2010) (cit. on p. 14).

[48] Anderson John. *Fundamentals of Aerodynamics, 6^{th} Edition*. Ed. by McGraw-Hill Education. 2017 (cit. on p. 7).

[49] Lohse Detlef. «Bubble puzzles: From fundamentals to applications». In: *Phys. Rev. Fluids* 3 (2018) (cit. on pp. 16, 47).

[50] Merle Frank, Raphaël Pierre, Rodnianski Igor, and Szeftel Jeremie. «On blow up for the energy super critical defocusing nonlinear Schrodinger equations». In: (2019) (cit. on pp. 20, 22, 26).

[51] Merle Frank, Raphaël Pierre, Rodnianski Igor, and Szeftel Jeremie. «On smooth self-similar solutions to the compressible Euler equations». In: (2019) (cit. on pp. 20, 22, 46).

[52] Merle Frank, Raphaël Pierre, Rodnianski Igor, and Szeftel Jeremie. «On the implosion of a three dimensional compressible fluid». In: (2019) (cit. on pp. 20, 22–25, 36, 42, 46).

[53] Canfarini R. *Personal photographic collection* (cit. on pp. 3, 65–69).

[54] Wills T. *Resin from Pinus Radiata Stump 3* (cit. on p. 70).

[55] Prosperetti A. «Thermal effects and damping mechanisms in the forced radial oscillations of gas bubbles in liquid». In: *J. Acoust. Soc. Am.* 61 (1977c), pp. 17–27 (cit. on p. 18).

[56] Eberlein C. «Sonoluminescence as quantum vacuum radiation». In: *Phys. Rev. Lett.* 76 (1996a), pp. 3842–3845 (cit. on p. 5).

[57] Eberlein C. «Theory of quantum radiation observed as sonoluminescence». In: *Phys. Rev. A* 53 (1996b), pp. 2772–2787 (cit. on p. 5).

[58] Yasui K. «Alternative model of single-bubble sonoluminescence». In: *Phys. Rev. E* 56 (1997a), pp. 6750–6760 (cit. on p. 18).

[59] Hilgenfeldt S., Grossmann S., and Lohse D. «A simple explanation of light emission in sonoluminescence». In: *Nature* 398 (1999a), pp. 402–405 (cit. on p. 18).

[60] Hilgenfeldt S., Grossmann S., and Lohse D. «Sonoluminescence light emission». In: *Phys. Fluids* 11 (1999b), pp. 1318–1330 (cit. on p. 18).